Although the previous studies reported the selective association of mood with spatial WM in an opposite manner to that with verbal WM (Bartolic et al., 1999; Gray, 2001), we did not observed a significant relationship between mood and PFC activity for the spatial WM task. One possibility causing this result is the individual variations in strategy use during the spatial WM task. In the verbal WM task, we used different Japanese morphograms (i.e., Hiragana/Katakana) for target (S1) and probe (S2) stimuli to prompt participants to use a verbal-phonological strategy rather than a visuospatial strategy (Smith et al., 1996). However, the spatial WM task used in our study allowed participants to use either a verbal or spatial strategy because the location of the target stimuli can be remembered by verbal labels (e.g., a number corresponding to each location), as discussed in previous studies (Nystrom et al., 2000). Cortical recruitment during WM tasks is known to depend on strategy use (Glabus et al., 2003). Thus, the homogeneity of strategy use (verbal or spatial) across participants conceivably made the relationship between mood and PFC activity unclear for the spatial WM task. One potential solution is to control the strategy use across participants in future research by using different task paradigms or by providing explicit instructions for memory strategy.

The underlying neural mechanisms of the selective interaction between mood and cognition are still unclear. Some researchers have proposed a "prefrontal asymmetry" hypothesis (Gray, 2001; Gray et al., 2002; Shackman et al., 2006). This hypothesis argues that positive (approach-related) and negative (withdrawal-related) affects are predominantly associated with the left and right hemispheres, respectively, whereby different affects are selectively related to cognitive functions linked with each hemisphere (e.g., verbal-left and spatial-right). However, incorporating our results with this hypothesis is difficult because we did not find clear evidence suggesting hemispheric asymmetry. Another account of the selective interaction between mood and cognition is based on pharmacological evidence. Animal studies have shown that certain cognitive functions involving the PFC (e.g., attentional set-shifting and reversal learning) are distinctly controlled by different neurotransmitters such as dopamine and serotonin (Robbins and Roberts, 2007). Because dopamine and serotonin have been suggested to be associated with positive and negative moods (Mitchell and Phillips, 2007), these transmitters could intermediate the selective interaction between moods and cognitive functions.

It should be noted that previous findings concerning the difference in mood-cognition interaction across cognitive functions remain inconsistent, possibly resulting from the variances in the task paradigms and the mood induction procedures (Shackman et al., 2006). In addition, we found a small but significant difference in accuracy between the tasks, suggesting slightly higher difficulty in the spatial WM tasks than the verbal WM task. This makes it difficult to interpret why we observed the between-task difference in the relationship between mood and PFC activity. Further investigation is needed to illuminate the possible difference between verbal and spatial WM in relation to mood under natural circumstances.

4.3. Limitations

Although we showed that the correlation between negative mood and the PFC activity during the verbal WM task was significant after controlling for age, gender, and task performance, several other factors could still mediate the relationship between mood and PFC activity. For example, this study did not assess or control participants' intelligence. Measures such as intelligence quotient (IQ) or fluid intelligence (gF) are known to be associated with both mood states and PFC activity during WM tasks (Gray et al., 2003; Samuel, 1980). These studies have shown that higher IQ is associated with lower negative moods and that greater gF is associated with more PFC activation during WM tasks. Thus, our results

could imply that higher intelligence mediates an inverse relationship between negative moods and PFC activation during the verbal WM task. Another concern is the relationship between naturalistic moods and personality traits. The experimental framework of the present study (i.e., individual-differences approach) precludes us from determining whether the observed relationship between mood and PFC activity derived from state-dependent factors (day-to-day fluctuations in mood states within an individual) or trait-like factors ('dispositional moods' persistent across time). Although the POMS questionnaire we used to evaluate the participants' naturalistic moods is considered to evaluate the responders' typical mood states rather than their personality traits (McNair and Heuchert, 2003), the participants' naturalistic moods under their current life situations may depend on their personality traits (Davidson, 2004; Kosslyn et al., 2002). This does not contradict previous fMRI studies suggesting the link between personality traits and PFC activity in response to WM tasks (DeYoung et al., 2009; Kumari et al., 2004). Meanwhile, several experiments have indicated that mood changes within individuals are indeed associated with PFC activity during cognitive tasks (Harrison et al., 2009; Liston et al., 2009). Thus, state-dependent mood factors apart from individual trait factors might at least in part have contributed to our results. To dissociate the contributions of state and trait factors to PFC activity, we need to administer multiple questionnaires for both state and trait measurement (Canli et al., 2004) or to use a within-subject design in which the PFC activity of individual participants is measured over multiple occasions.

5. Conclusion

Our study demonstrated that naturalistic moods in healthy people are related to PFC activity during a verbal WM task. We showed that this relationship remained significant even after controlling for potential confounding factors such as age, gender, and task performance. One thing of note is that a mild variation of naturalistic negative moods among healthy people can be associated with PFC activity even absent experimental affective modulation. The relationship between negative mood and verbal WM in the PFC is particularly of interest, considering clinical findings showing PFC impairment during verbal WM tasks in mood disorders such as major depression (Harvey et al., 2005; Matsuo et al., 2007; Siegle et al., 2007). Further research will lead to more comprehensive understanding of the mood-cognition interaction under broader contexts, bridging the gap across induced moods and naturalistic moods among healthy people, as well as pathological moods in patients with mood disorders.

Appendix A. Supplementary data

Supplementary data associated with this article can be found, in the online version, at doi:10.1016/j.neures.2011.02.011.

References

Anticevic, A., Repovs, G., Barch, D.M., 2010. Resisting emotional interference: brain regions facilitating working memory performance during negative distraction. Cogn. Affect. Behav. Neurosci. 10, 159–173.
Ashby, F.G., Isen, A.M., Turken, A.U., 1999. A neuropsychological theory of positive affect and its influence on cognition. Psychol. Rev. 106, 529–550.
Baddeley, A., 2003. Working memory: looking back and looking forward. Nat. Rev. Neurosci. 4, 829–839.

Bartolic, E.I., Basso, M.R., Schefft, B.K., Glauser, T., Titanic-Schefft, M., 1999. Effects of experimentally-induced emotional states on frontal lobe cognitive task performance. Neuropsychologia 37, 677–683.

Canli, T., Amin, Z., Haas, B., Omura, K., Constable, R.T., 2004. A double dissociation between mood states and personality traits in the anterior cingulate. Behav. Neurosci. 118, 897–904.

Davidson, R.J., 2004. Well-being and affective style: neural substrates and biobehavioural correlates. Philos. Trans. R. Soc. Lond. B Biol. Sci. 359, 1395–1411.

DeYoung, C.G., Shamosh, N.A., Green, A.E., Braver, T.S., Gray, J.R., 2009. Intellect as distinct from Openness: differences revealed by fMRI of working memory. J. Pers. Soc. Psychol. 97, 883–892.

Eriksen, B.A., Eriksen, C.W., 1974. Effects of noise letters upon the identification of a target letter in a nonsearch task. Percept. Psychophys. 16, 143–149.

Glabus, M.F., Horwitz, B., Holt, J.L., Kohn, P.D., Gerton, B.K., Callicott, J.H., Meyer-Lindenberg, A., Berman, K.F., 2003. Interindividual differences in functional interactions among prefrontal, parietal and parahippocampal regions during working memory. Cereb. Cortex 13, 1352–1361.

Gray, J.R., 2001. Emotional modulation of cognitive control: approach-withdrawal states double-dissociate spatial from verbal two-back task performance. J. Exp. Psychol. Gen. 130, 436–452.

Gray, J.R., Braver, T.S., Raichle, M.E., 2002. Integration of emotion and cognition in the lateral prefrontal cortex. Proc. Natl. Acad. Sci. U.S.A. 99, 4115–4120.

Gray, J.R., Chabris, C.F., Braver, T.S., 2003. Neural mechanisms of general fluid intelligence. Nat. Neurosci. 6, 316–322.

Harrison, N.A., Brydon, L., Walker, C., Gray, M.A., Steptoe, A., Dolan, R.J., Critchley, H.D., 2009. Neural origins of human sickness in interoceptive responses to inflammation. Biol. Psychiatry 66, 415–422.

Harvey, P.O., Fossati, P., Pochon, J.B., Levy, R., Lebastard, G., Lehericy, S., Allilaire, J.F., Dubois, B., 2005. Cognitive control and brain resources in major depression: an fMRI study using the n-back task. NeuroImage 26, 860–869.

Herrmann, M.J., Walter, A., Schreppel, T., Ehlis, A.C., Pauli, P., Lesch, K.P., Fallgatter, A.J., 2007. D4 receptor gene variation modulates activation of prefrontal cortex during working memory. Eur. J. Neurosci. 26, 2713–2718.

Hoshi, Y., Tsou, B.H., Billock, V.A., Tanosaki, M., Iguchi, Y., Shimada, M., Shinba, T., Yamada, Y., Oda, I., 2003. Spatiotemporal characteristics of hemodynamic changes in the human lateral prefrontal cortex during working memory tasks. NeuroImage 20, 1493–1504.

Kameyama, M., Fukuda, M., Yamagishi, Y., Sato, T., Uehara, T., Ito, M., Suto, T., Mikuni, M., 2006. Frontal lobe function in bipolar disorder: a multichannel near-infrared spectroscopy study. NeuroImage 29, 172–184.

Kosslyn, S.M., Cacioppo, J.T., Davidson, R.J., Hugdahl, K., Lovallo, W.R., Spiegel, D., Rose, R., 2002. Bridging psychology and biology. The analysis of individuals in groups. Am. Psychol. 57, 341–351.

Kumari, V., ffytche, D.H., Williams, S.C., Gray, J.A., 2004. Personality predicts brain responses to cognitive demands. J. Neurosci. 24, 10636–10641.

Liston, C., McEwen, B.S., Casey, B.J., 2009. Psychosocial stress reversibly disrupts prefrontal processing and attentional control. Proc. Natl. Acad. Sci. U.S.A. 106, 912–917.

Luciana, M., Collins, P.F., Depue, R.A., 1998. Opposing roles for dopamine and serotonin in the modulation of human spatial working memory functions. Cereb. Cortex 8, 218–226.

Maki, A., Yamashita, Y., Ito, Y., Watanabe, E., Mayanagi, Y., Koizumi, H., 1995. Spatial and temporal analysis of human motor activity using noninvasive NIR topography. Med. Phys. 22, 1997–2005.

Martin, M., 1990. On the induction of mood. Clin. Psychol. Rev. 10, 669–697.

Matsuo, K., Glahn, D.C., Peluso, M.A., Hatch, J.P., Monkul, E.S., Najt, P., Sanches, M., Zamarripa, F., Li, J., Lancaster, J.L., Fox, P.T., Gao, J.H., Soares, J.C., 2007. Prefrontal hyperactivation during working memory task in untreated individuals with major depressive disorder. Mol. Psychiatry 12, 158–166.

Mayer, J.D., McCormick, L.J., Strong, S.E., 1995. Mood-congruent memory and natural mood: new evidence. Pers. Soc. Psychol. Bull. 21, 736–746.

McNair, D.M., Heuchert, J.P., 2003. Profile of Mood States Technical Update. Multi-Health Systems, New York.

McNair, P.M., Lorr, M., Droppleman, L.F., 1971. Profile of Mood States Manual. Educational and Industrial Testing Service, San Diego.

Minagawa-Kawai, Y., van der Lely, H., Ramus, F., Sato, Y., Mazuka, R., Dupoux, E., 2011. Optical brain imaging reveals general auditory and language-specific processing in early infant development. Cereb. Cortex 21, 254–261.

Mitchell, R.L., Phillips, L.H., 2007. The psychological, neurochemical and functional neuroanatomical mediators of the effects of positive and negative mood on executive functions. Neuropsychologia 45, 617–629.

Nystrom, L.E., Braver, T.S., Sabb, F.W., Delgado, M.R., Noll, D.C., Cohen, J.D., 2000. Working memory for letters, shapes, and locations: fMRI evidence against stimulus-based regional organization in human prefrontal cortex. NeuroImage 11, 424–446.

Okamoto, M., Dan, I., 2005. Automated cortical projection of head-surface locations for transcranial functional brain mapping. NeuroImage 26, 18–28.

Oldfield, R.C., 1971. The assessment and analysis of handedness: the Edinburgh inventory. Neuropsychologia 9, 97–113.

Orihuela-Espina, F., Leff, D.R., James, D.R., Darzi, A.W., Yang, G.Z., 2010. Quality control and assurance in functional near infrared spectroscopy (fNIRS) experimentation. Phys. Med. Biol. 55, 3701–3724.

Papousek, I., Schulter, G., Lang, B., 2009. Effects of emotionally contagious films on changes in hemisphere-specific cognitive performance. Emotion 9, 510–519.

Parrot, W.G., Sabini, J., 1990. Mood and memory under natural conditions: evidence for mood incongruent recall. J. Pers. Soc. Psychol. 59, 321–336.

Pena, M., Maki, A., Kovacic, D., Dehaene-Lambertz, G., Koizumi, H., Bouquet, F., Mehler, J., 2003. Sounds and silence: an optical topography study of language recognition at birth. Proc. Natl. Acad. Sci. U.S.A. 100, 11702–11705.

Perlstein, W.M., Elbert, T., Stenger, V.A., 2002. Dissociation in human prefrontal cortex of affective influences on working memory-related activity. Proc. Natl. Acad. Sci. U.S.A. 99, 1736–1741.

Qin, S., Hermans, E.J., van Marle, H.J., Luo, J., Fernandez, G., 2009. Acute psychological stress reduces working memory-related activity in the dorsolateral prefrontal cortex. Biol. Psychiatry 66, 25–32.

Robbins, T.W., Roberts, A.C., 2007. Differential regulation of fronto-executive function by the monoamines and acetylcholine. Cereb. Cortex 17, i151–i160.

Robinson, O.J., Sahakian, B.J., 2009. A double dissociation in the roles of serotonin and mood in healthy subjects. Biol. Psychiatry 65, 89–92.

Samuel, W., 1980. Mood and personality correlates of IQ by race and sex of subject. J. Pers. Soc. Psychol. 38, 993–1004.

Sato, H., Fuchino, Y., Kiguchi, M., Katura, T., Maki, A., Yoro, T., Koizumi, H., 2005. Intersubject variability of near-infrared spectroscopy signals during sensorimotor cortex activation. J. Biomed. Opt. 10, 44001.

Sato, H., Takeuchi, T., Sakai, K.L., 1999. Temporal cortex activation during speech recognition: an optical topography study. Cognition 73, B55–B66.

Schroeter, M.L., Zysset, S., Wahl, M., von Cramon, D.Y., 2004. Prefrontal activation due to Stroop interference increases during development–an event-related fNIRS study. NeuroImage 23, 1317–1325.

Shackman, A.J., Sarinopoulos, I., Maxwell, J.S., Pizzagalli, D.A., Lavric, A., Davidson, R.J., 2006. Anxiety selectively disrupts visuospatial working memory. Emotion 6, 40–61.

Siegle, G.J., Thompson, W., Carter, C.S., Steinhauer, S.R., Thase, M.E., 2007. Increased amygdala and decreased dorsolateral prefrontal BOLD responses in unipolar depression: related and independent features. Biol. Psychiatry 61, 198–209.

Singh, A.K., Dan, I., 2006. Exploring the false discovery rate in multichannel NIRS. NeuroImage 33, 542–549.

Singh, A.K., Okamoto, M., Dan, H., Jurcak, V., Dan, I., 2005. Spatial registration of multichannel multi-subject fNIRS data to MNI space without MRI. NeuroImage 27, 842–851.

Smith, E.E., Jonides, J., 1999. Storage and executive processes in the frontal lobes. Science 283, 1657–1661.

Smith, E.E., Jonides, J., Koeppe, R.A., 1996. Dissociating verbal and spatial working memory using PET. Cereb. Cortex 6, 11–20.

Suda, M., Fukuda, M., Sato, T., Iwata, S., Song, M., Kameyama, M., Mikuni, M., 2009. Subjective feeling of psychological fatigue is related to decreased reactivity in ventrolateral prefrontal cortex. Brain Res. 1252, 152–160.

Suda, M., Sato, T., Kameyama, M., Ito, M., Suto, T., Yamagishi, Y., Uehara, T., Fukuda, M., Mikuni, M., 2008. Decreased cortical reactivity underlies subjective daytime light sleepiness in healthy subjects: a multichannel near-infrared spectroscopy study. Neurosci. Res. 60, 319–326.

Suto, T., Fukuda, M., Ito, M., Uehara, T., Mikuni, M., 2004. Multichannel near-infrared spectroscopy in depression and schizophrenia: cognitive brain activation study. Biol. Psychiatry 55, 501–511.

Takizawa, R., Kasai, K., Kawakubo, Y., Marumo, K., Kawasaki, S., Yamasue, H., Fukuda, M., 2008. Reduced frontopolar activation during verbal fluency task in schizophrenia: a multi-channel near-infrared spectroscopy study. Schizophr. Res. 99, 250–262.

Tsujimoto, S., Yamamoto, T., Kawaguchi, H., Koizumi, H., Sawaguchi, T., 2004. Prefrontal cortical activation associated with working memory in adults and preschool children: an event-related optical topography study. Cereb. Cortex 14, 703–712.

Yokoyama, K., Araki, S., Kawakami, N., Takeshita, T., 1990. Production of the Japanese edition of profile of mood states (POMS): assessment of reliability and validity. Nippon Koshu Eisei Zasshi 37, 913–918.

Mitochondrial adaptations in skeletal muscle to hindlimb unloading

Akira Wagatsuma · Naoki Kotake ·
Takayuki Kawachi · Masataka Shiozuka ·
Shigeru Yamada · Ryoichi Matsuda

Abstract To gain insight into the regulation of mitochondrial adaptations to hindlimb unloading (HU), the activity of mitochondrial enzymes and the expression of nuclear-encoded genes which control mitochondrial properties in mouse gastrocnemius muscle were investigated. Biochemical and enzyme histochemical analysis showed that subsarcolemmal mitochondria were lost largely than intermyofibrillar mitochondria after HU. Gene expression analysis revealed disturbed or diminished gene expression patterns. The three main results of this analysis are as follows. First, in contrast to peroxisome proliferator-activated receptor γ coactivator 1 β (PGC-1β) and PGC-1-related coactivator, which were down-regulated by HU, PGC-1α was up-regulated concomitant with decreased expression of its DNA binding transcription factors, PPARα, and estrogen-related receptor α (ERRα). Moreover, there was no alteration in expression of nuclear respiratory factor 1, but its downstream target gene, mitochondrial transcription factor A, was down-regulated. Second, both mitofusin 2 and fission 1, which control mitochondrial morphology, were down-regulated. Third, ATP-dependent Lon protease, which participates in mitochondrial-protein degradation, was also down-regulated. These findings suggest that HU may induce uncoordinated expression of PGC-1 family coactivators and DNA binding transcription factors, resulting in reducing ability of mitochondrial biogenesis. Furthermore, down-regulation of mitochondrial morphology-related genes associated with HU may be also involved in alterations in intracellular mitochondrial distribution.

Keywords Adaptation · Atrophy · Hindlimb unloading · Mitochondria · Skeletal muscle

A. Wagatsuma (✉) · T. Kawachi · M. Shiozuka · S. Yamada ·
R. Matsuda
Department of Life Sciences, Graduate School of Arts and
Sciences, The University of Tokyo, 3-8-1 Komaba,
Meguro-ku, Tokyo, Japan
e-mail: wagatsuma1969@yahoo.co.jp

N. Kotake
Department of Advanced Interdisciplinary Studies (AIS),
Graduate School of Engineering, The University of Tokyo,
4-6-1 Komaba, Meguro-ku, Tokyo, Japan

Introduction

Mitochondria play important roles in energy homeostasis, metabolism, signaling, and apoptosis [1]. The abundance, morphology, and functional properties of mitochondria are dynamically regulated in response to alterations in neuromuscular activity. Basically, physical activity (e.g., exercise, endurance training, and interval training) promotes mitochondrial biogenesis, [2] whereas disuse (e.g., denervation, immobilization, spaceflight, and hindlimb unloading) discourages mitochondrial biogenesis [3–5].

A model of hindlimb unloading (HU) of a rodent is frequently used to simulate and study neuromuscular perturbations occurring in a real microgravity environment during spaceflights [6]. This earth-based model of microgravity is characterized by reduction of motor activity and lack of load bearing [7]. The major modifications concerning HU are muscle atrophy [4] and slow-to-fast fiber-type switching [7]. In addition, experimental evidence for mitochondrial adaptations to HU is accumulating; for example, mitochondrial fragmentation [8], decreased mitochondrial enzyme activity [9–14], and reduced mitochondrial oxygen consumption [9] have been reported. However, these adaptive mechanisms concerning HU remain to be elucidated. Understanding these adaptive

mechanisms may extend our knowledge of skeletal muscle plasticity and provide important insights into both space-flight- and earth-based health problems.

The adaptive mechanisms may be associated with transcriptional alterations in expression of mitochondrial biogenesis-related and other mitochondria-related genes. Mitochondrial biogenesis is a complex biological process that requires the system to import and incorporate proteins and lipids into the existing mitochondrial reticulum as well as to replicate mitochondrial DNA (mtDNA) [1]. The transcriptional mechanism that controls mitochondrial biogenesis is a complex network. The peroxisome prolif-erator-activated receptor, γ, coactivator 1 (PGC-1) family of transcriptional coactivators interact with multiple DNA binding transcription factors to coordinate the regulation of multiple mitochondrial genes [1]. PGC-1α coactivates expression of estrogen-related receptor α (ERRα), which activates expression of peroxisome proliferator-activated receptor α (PPARα), nuclear respiratory factor 1 (NRF-1), and NRF-2 [15]. NRF-1 activates expression of oxidative phosphorylation components, mitochondrial transporters, and mitochondrial ribosomal proteins [1]. In addition, NRF-1 regulates expression of mitochondrial transcription factor A (TFAM), contributing to mtDNA replication and transcription [16]. Apart from mitochondrial biogenesis, a recent report has highlighted the importance of mitochon-drial dynamics in cell and animal physiology. Mitochon-dria constantly fuse and divide, and an imbalance of these two processes dramatically alters overall mitochondrial morphology and function [17]. Mitochondrial fission is driven by dynamin 1-like and fission 1, while mitochon-drial fusion is controlled by mitofusins and OPA 1 [18]. Moreover, ATP-dependent Lon protease is known to cat-alyze the degradation of oxidatively modified matrix pro-teins [19]. These nuclear-encoded genes which control mitochondrial properties may therefore be key contributors to mitochondrial adaptations to HU.

In this study, we hypothesize that mitochondrial adapta-tions to HU are due, at least in part, to transcriptional altera-tions in expression of nuclear-encoded genes which control mitochondrial properties. To test this hypothesis, we investi-gated the activity of mitochondrial enzymes and the expres-sion of nuclear-encoded genes involved in mitochondrial biogenesis, mitochondrial morphogenesis, and mitochondrial-protein degradation in mouse gastrocnemius muscle.

Materials and methods

Animals

Female seven-week-old CD1 mice (Clea Japan, Meguro, Tokyo) were used and housed in the animal care facility

under a 12-h light/12-h dark cycle at room temperature (23 $\pm$ 2°C) and 55 $\pm$ 5% humidity. Mice were matched by body weight and then assigned to one of two groups as follows: ground-based control ($n = 12$) or HU ($n = 12$). The mice were procured after approval for this study from The University of Tokyo Animal Ethics Committee.

Preparation of mitochondria population

Two mitochondrial fractions, termed subsarcolemmal (SS) and intermyofibrillar (IMF) mitochondria, were isolated from skeletal muscle as previously reported [20]. Briefly, the skeletal muscle (the deep-red region of the gastrocne-mius) was removed and immediately placed in ice-cold isolation buffer (IB). The muscles were freed of fat and connective tissue, transferred into fresh IB, and weighed. All further procedures were carried out at 0–5°C. The muscle sample was next minced with triple scissors in IB. The muscle sample was homogenized by using a tissue homogenizer for 10 s. The homogenate was centrifuged at 800g for 10 min, and the resulting precipitate was subse-quently used for the preparation of the IMF mitochondria. The final SS mitochondrial pellet was suspended in IB. The pellet from the 800g centrifugation contained primarily intact material with some remaining SS mitochondria. This pellet was then washed, and the IMF mitochondria were liberated with nagarse incubation. After two washes were performed, the final IMF mitochondrial pellet was sus-pended in IB. The final mitochondrial protein concentration was determined by a micro bicinchoninic acid (BCA) assay (Pierce Chemical Co., Rockford, IL) with bovine serum albumin as a standard.

Procedure for hindlimb unweighting

A rat-hindlimb-suspension model, originally described in [21], was modified for use with mice [22]. Briefly, each mouse was weighed and anesthetized with an intraperito-neal injection of pentobarbital (50 mg/kg body weight). We wrapped bandages (Nichiban, Bunkyo, Tokyo) around the tail of the mice. After the mouse had recovered from the anesthetic, a swivel hook was placed through the bandage distal to the tip of the tail. This method allows the animals full 360° rotation as well as access to food and water without allowing the hindlimbs to contact the cage floor or walls. HU was continued for 7 days. All the pro-cedures in the animal experiments were carried out in accordance with the guidelines presented in the Guiding Principles for the Care and Use of Animals in the Field of Physiological Sciences, published by the Physiological Society of Japan.

Enzyme activity assay

The activity of citrate synthase (CS) was determined spectrophotometrically according to Srere [23]. Briefly, skeletal muscle (the deep-red region of the gastrocnemius) was homogenized in 175 mM KCl, 10 mM GSH, and 2 mM EDTA at pH 7.4. The homogenate thus obtained was frozen and thawed four times and mixed thoroughly before enzymatic measurements were performed. The principle of the assay is to initiate the reaction of acetyl-CoA with oxaloacetate and the link the release of free CoA-SH to a colorimetric reagent, 5,5-dithiobis-(2-nitrobenzoate) (DTNB). The absorbance of the reaction mixtures was monitored at wavelength of 405 nm at 15 s intervals for a period of 3 min. The activity of 3-hydroxyacyl-CoA dehydrogenase (3-HAD) was assayed by measuring the decrease in absorbance at 340 nm due to the oxidation of NADH in the presence of acetoacetyl-CoA as described [24]. The absorbance of the reaction mixtures was monitored at 15 s intervals for a period of 5 min. The enzyme activities were normalized in regard to wet weight of skeletal muscle.

Enzyme histochemical analysis

To examine mitochondrial location in a myofiber, succinate dehydrogenase (SDH) staining was carried out according to Nachlas et al. [25] with minor modification. Briefly, frozen transverse sections from the mid-belly region of the gastrocnemius muscles were incubated for 10 min at 37°C in a medium (0.9 mM 1-methoxyphenazine methylsulfate, 1.5 mM nitro blue tetrazolium, 5.6 mM EDTA, and 48 mM succinate disodium salt at pH 7.6) in a 0.1 M phosphate buffer, rinsed for 5 min with deionized H_2O, dehydrated for 5 min within a myofiber in 50% acetone, and then air-dried. The fiber cross-sectional area (FCSA) and length of SDH activity wit were measured by using ImageJ software (ver. 1.42, http://rsb.info.nih.gov/ij/).

Gene expression analysis

Total RNA was prepared with TRI reagent (Molecular Research Center, Cincinnati, OH). The DNase-treated total RNA was converted to cDNA by using a first-strand cDNA synthesis system for quantitative RT-PCR (Marligen, Biosciences, Ijamsville, MD). The cDNA samples were aliquoted and stored at −80°C. Real-time PCR was carried out using an Opticon™ DNA engine (MJ Research, Waltham, MA) according to the manufacturer's instructions. The reactions employed gene-specific primers for citrate synthase, mitofusin 2, fission1, Lon protease (Takara Bio Inc., Otsu, Shiga), succinate dehydrogenase [26], medium-chain acyl-coenzyme A dehydrogenase (MCAD) [27], peroxisome proliferator-activated receptor, γ, coactivator

1α (PGC-1α), peroxisome proliferator-activated receptor, γ, coactivator 1β (PGC-1β) [28], peroxisome proliferator-activated receptor, γ, coactivator-related 1 (PRC), PPARα [29], mitochondrial transcription factor A (TFAM), mitochondrial single-stranded DNA binding protein 1 (mtSSB) [30], NRF-1, NRF-2 [31], ERRα [32], and manganese superoxide dismutase (MnSOD) [33]. PCR thermal-cycle conditions were optimized to achieve a single ethidium bromide-stained band following electrophoresis on a 2% agarose gel. Differences in gene expression were calculated relative to the expression of a housekeeping gene by comparison with a standard curve. To identify the appropriate housekeeping gene, we investigated several housekeeping genes including 18S ribosomal RNA, glyceraldehyde-3-phosphate dehydrogenase, β-actin, and cyclophilin. We selected cyclophilin as the housekeeping gene because its expression levels remain unchanged in hindlimb-unloaded muscle relative to control muscle. Cyclophilin was found to be appropriate for normalizing the signal by comparing the differences in raw threshold cycle values (i.e., the number of amplification cycles at which the signal is detected above the background and is in the exponential phase). A standard curve was constructed from serially diluted cDNA of gastrocnemius muscle. Each sample was normalized by its cyclophilin content. The final results were expressed as a relative fold change compared to that of control animals.

Statistics

Data are means ± SEM. For analysis between the control and HU cases, Student's t test was used to determine significance. The level of significance was set at $P < 0.05$.

Results

To assess whether the mouse model mimics the rat model previously reported, the degree of muscle atrophy was estimated, and the expression of atrogin-1 mRNA, muscle-specific ubiquitin-ligase, which is known to mediate rodent muscle atrophy, was investigated. Myofibers from hindlimb-unloaded mice were pathologically atrophied in reference to those from control mice. Significant decreases in the FCSA of two types of myofiber (52% for SDH^{High} and 51% for SDH^{Low}) were observed after 7 days of HU. Moreover, atrogin-1 mRNA transcript was strongly induced in the HU case compared to the control case (Fig. 1).

Subsarcolemmal mitochondria were degraded more rapidly than IMF mitochondria during HU [8]. Therefore, we isolated SS and IMF mitochondria from control and hindlimb-unloaded mice. As expected, SS mitochondria
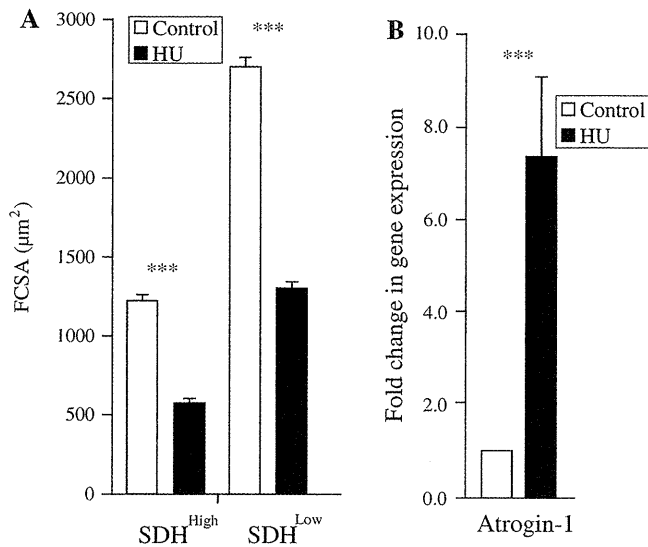
Fig. 1 Effects of HU on myofiber size and mRNA expression levels of atrogin-1, a muscle-specific ubiquitin-ligase required for muscle atrophy. **a** After 7 days of HU, muscle tissues were cryosectioned and reacted for SDH activity. Myofibers were divided into two groups: SDH^{High} (dark stain) and SDH^{Low} (light stain). FCSA was measured with the image-analysis system, calibrated to transform the number of pixels (viewed on a computer monitor) into micrometers. **b** To investigate mRNA expression levels between control and HU, total RNA was isolated from muscle tissues and relative gene expression was quantified by real-time PCR. Cyclophilin was used internal control. The data are means ± SEM ($n = 6$). Statistically significant differences compared to control: ***$P < 0.001$

Fig. 2 Effects of HU on quantitative alteration in mitochondria in SS and IMF regions of muscle fibers. SS and IMF mitochondrial fractions were isolated from control and hindlimb-unloaded mice by differential centrifugation and digestion techniques. Mitochondrial protein content was determined using micro BCA assay and the yield was expressed as mg/g tissue weight. The data are means ± SEM ($n = 6$). Statistically significant differences compared to control: **$P < 0.01$

were significantly decreased in the HU case compared to that in the control case. Although IMF mitochondria also showed a tendency to decrease after HU, there was no significant difference between groups (Fig. 2).

Because HU decreases the activity of mitochondrial enzymes, the activity of CS was measured. The activity was significantly decreased in the HU case compared to that in the control case. It has been reported that HU suppressed gene expression of enzyme in fatty-acid oxidation [34]. Therefore, we measured the activity of 3-HAD, a key enzyme in muscle fatty-acid oxidation. The activity was significantly decreased in the HU case compared to that in the control case. CS and MCAD mRNA transcripts levels were significantly decreased in the HU case compared to that in the control case.

To examine whether HU affects the location-specific differences in mitochondrial enzyme activity, an enzyme histochemical SDH staining on cryosections was carried out. SDH activity in SS and IMF regions in the control and hindlimb-unloaded mice was observed (Fig. 3a). The area of SS SDH activity in SDH^{High} myofibers was measured. The SS SDH activity was significantly decreased in the HU case compared to the control case, whereas ratio of SDH activity area to FCSA was insignificantly decreased slightly (Fig. 3b). Furthermore, the length of SS SDH
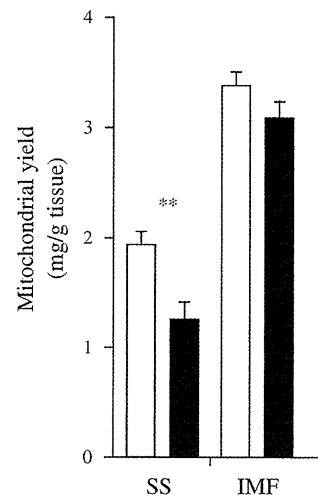
activity in SDH^{High} myofiber was measured. This measurement shows that the length was significantly decreased in the HU case compared to the control case (Fig. 3c). Next, the area of IMF SDH activity in SDH^{High} myofibers was measured. The SDH activity was significantly decreased in the HU case compared to the control case, whereas the ratio of SDH activity area to FCSA was significantly increased (Fig. 3d). In addition, SDH mRNA transcript level was significantly decreased in the HU case compared to the control case (Fig. 3e).

To examine the effects of HU on expression of mitochondrial biogenesis-related genes, RNA samples from the gastrocnemius of control and hindlimb-unloaded mice were subjected to cDNA synthesis and real-time PCR. The PGC-1 family, including PGC-1α, -1β, and PRC, is known to play a central role in mitochondrial biogenesis. PGC-1α mRNA transcript level was significantly increased in the HU case compared to the control case, whereas PGC-1β and PRC mRNA transcript levels were significantly decreased. The transcript level of DNA binding transcription factors, which interact with PGC-1 coregulators, was investigated. Both PPARα and ERRα mRNA transcripts levels were significantly decreased in the HU case compared to the control case. In contrast, NRF-1 mRNA transcript level was insignificantly decreased in the HU case compared to the control case, whereas NRF-2 mRNA transcript level was significantly increased. TFAM and mtSSB function as a key regulator of mammalian mtDNA maintenance. TFAM mRNA transcript level was significantly decreased in the HU case compared to the control
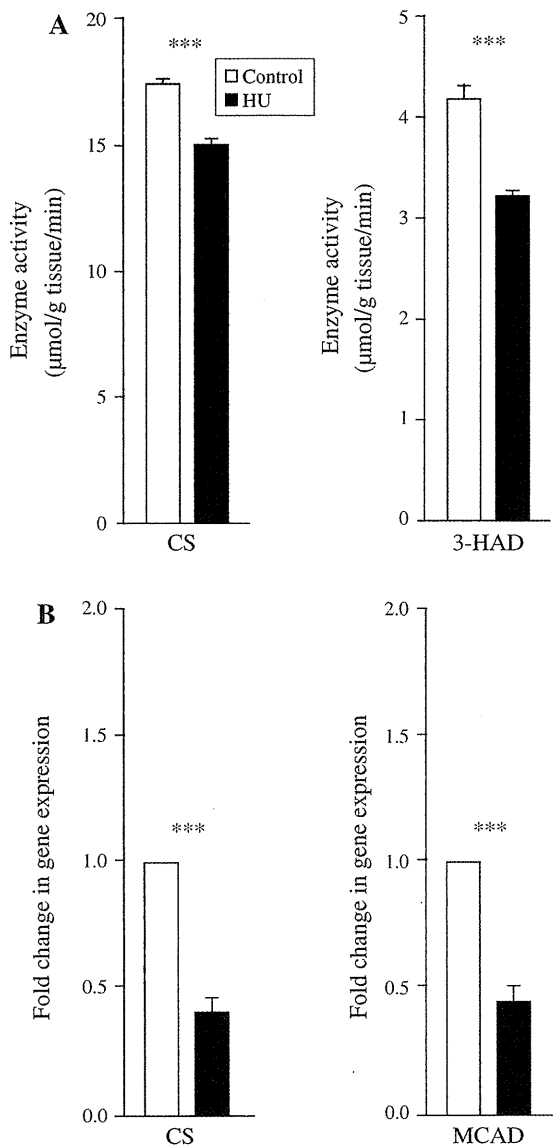
Fig. 3 Effects of HU on activities of mitochondrial enzymes and mRNA expression levels of mitochondrial enzymes. **a** The tissue homogenates were subjected to freeze-thaw cycles, centrifuged, and assayed for enzyme activities. The enzyme activity was normalized for wet weight of skeletal muscle. **b** Total RNA was prepared from muscle tissues and relative gene expression was determined by real-time PCR. The transcript levels were compared to control mice. The data are means ± SEM ($n = 6$). Statistically significant differences compared to control: ***$P < 0.001$

case, whereas mtSSB mRNA transcript level was significantly increased (Fig. 4).

The transcript level of two GTPase proteins that act in opposing fusion and fission pathways for maintaining the dynamic of tubular mitochondrial networks were investigated. Both mitofusin 2 mRNA and fission 1 mRNA transcripts levels were significantly decreased in the HU case compared to the control case. ATP-dependent Lon protease mRNA transcript level, which is implicated in mitochondrial protein degradation, was significantly

decreased in the HU case compared to the control case (Fig. 5).

Hindlimb unloading increases oxidative stress and disrupts antioxidant capacity in skeletal muscle [35]. MnSOD (localized in the mitochondrial matrix) provides a major defense against oxidative damage by reactive oxygen species (ROS). MnSOD mRNA transcript level remained unchanged in the HU case compared to the control case (Fig. 6).

Discussion

Mammalian mitochondria exhibit a remarkable capacity to adapt to physiological and pathophysiological demands. The processes by which these adaptations occur are thought to be largely achieved at the level of transcriptional regulation. Accordingly, this study focused on the activity of mitochondrial enzymes and the expression of nuclear-encoded genes involved in mitochondrial biogenesis, mitochondrial morphogenesis, and mitochondrial-protein degradation after HU. Our findings provide the insight that mitochondrial adaptations to HU may be associated with distorted gene expression, resulting in changes in the abundance, morphology, and functional properties of mitochondria.

The modified hindlimb suspension model was chosen because it is considered less stressful on the animal than the harness method. Differences in body weights throughout the experimental period can influence interpretation of the experimental results [6]. In our experiment, mice from the hindlimb-unloaded group showed no significant difference in body weight compared with the control group (data not shown), suggesting that the stress effects that occurred during 7 days of HU were minimal. To verify the efficiency of the HU, the changes in myofiber size after 7 days of HU were investigated. The degree of change in our experiment was greater than that in previously reported ones [36, 37]. This difference may be attributed largely to differences between the experimentation set-ups used in the laboratories concerned. The expression of atrogin-1, which is generally recognized as a molecular marker for muscle atrophy, was investigated. A strong up-regulation of atrogin-1 after HU, which is in line with previous reports [38–40], was observed. HU reduced the activity of mitochondrial enzymes as previously reported [9–14]. These findings demonstrate the reliability of our HU model.

Mitochondria that are clustered in proximity to the sarcolemma are termed SS mitochondria, and those embedded among myofibrils are called IMF mitochondria [41]. In this study, SS mitochondria were lost largely than IMF mitochondria after HU. This finding is in keeping with the previous report that the absolute volumes of SS and

Fig. 4 Regional differences in the mitochondrial adaptations to HU. **a** Histochemical staining for SDH activity was performed on cryosections of the gastrocnemius muscle. *Scale bar* = 50 μm. **b** Quantification of SS SDH staining area in a myofiber was measured with the image-analysis system, calibrated to transform the number of pixels into micrometers. Subsarcolemmal SDH staining area in a myofiber was normalized for FCSA. **c** Quantification of length of SS SDH staining was measured. **d** Quantification of IMF SDH staining area in a myofiber was measured. Intermyofibrillar SDH staining area in a myofiber was normalized for FCSA. **e** Total RNA was prepared from muscle tissues and relative gene expression was determined by real-time PCR. The data are means ± SEM ($n = 6$). Statistically significant differences compared to control: ***$P < 0.001$
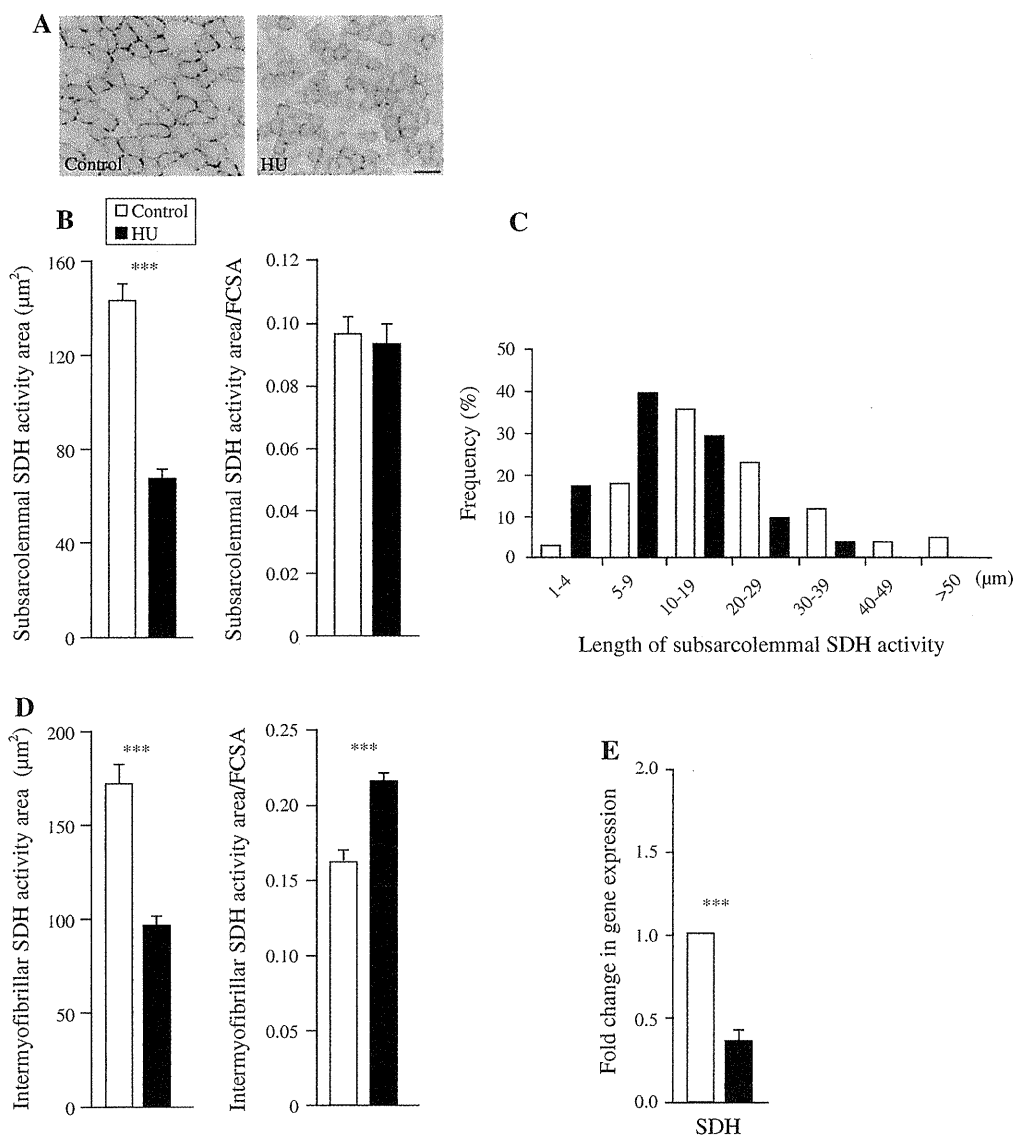
IMF mitochondria decrease by 73 and 45% after 5 weeks of hindlimb suspension [42]. We founded that SS mitochondria decreased in proportion to myofiber size but IMF mitochondria increased in proportion to myofiber size, suggesting that SS mitochondria were degraded more rapidly than IMF mitochondria. This phenomenon may be attributable to the development of autophagy. Riley et al. [8] indicated that autolytic degradation occurs during HU in light of the appearance of vacuolation and fragmentation of SS mitochondria.

The possible mechanism for regulating mitochondrial distribution in myofibers is not fully understood. However, it is hypothesized that abnormal distribution of mitochondria during microgravity may be due to disturbance of the structural integrity of mitochondria. In this regard, Nikawa et al. [43] reported that expression of A-kinase anchoring protein and cytoplasmic dynein, which are associated with the anchoring and movement of mitochondria, decreased in

spaceflight but not in tail-suspension tests. Indeed, they did not observe abnormal distribution of mitochondria in a tail-suspended rat. This result is inconsistent with previous reports [8, 42] and our present findings. We hypothesized that this phenomenon may be associated with changes in mitochondrial morphology. In this study, therefore, we focused attention on mitochondrial morphogenesis-related genes, namely, mitofusin 2 and fission 1. Consistent with the result presented in a previous report [8], the SS mitochondria (SDH activity) in the HU case were smaller in size than those in the control case (Fig. 7b, c). Moreover, expression of mitofusin 2 decreased after HU. This is a reasonable result because this gene is regulated by PGC-1β and ERRα [44], which are down-regulated by HU. This finding is partially supported by the observation that repression of mitofusin 2 in muscle cells shows a fragmentation of the mitochondrial network [45]. However, we did not observe up-regulation of fission 1, suggesting that
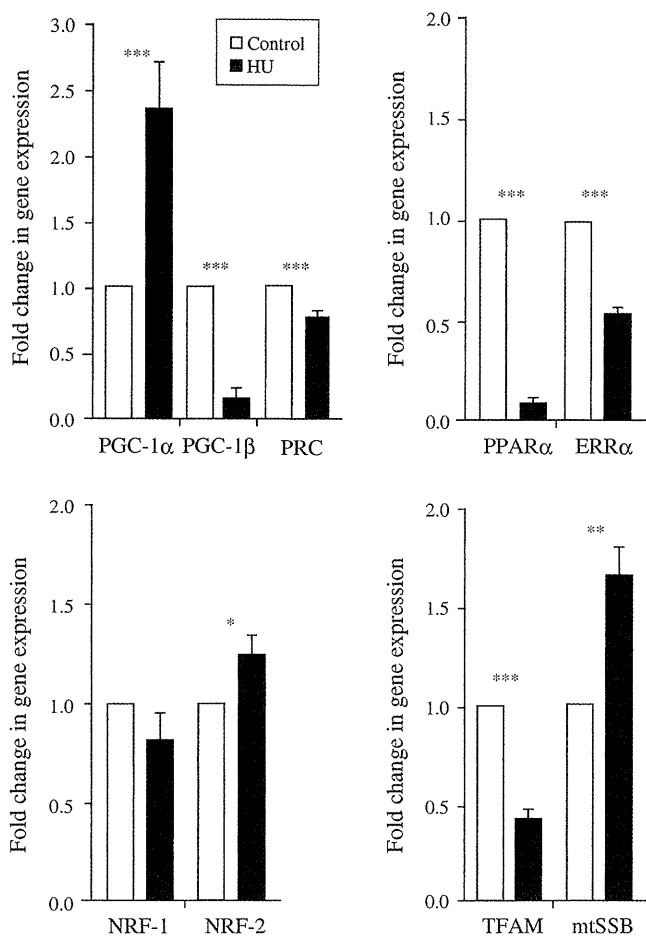
Fig. 5 Effects of HU on expression of mitochondrial biogenesis-related genes. Total RNA was prepared from muscle tissues and relative gene expression was determined by real-time PCR. The transcript levels were compared to control mice. The data are means ± SEM ($n = 6$). Statistically significant differences compared to control: $*P < 0.05$, $**P < 0.01$, and $***P < 0.001$

Fig. 6 Effects of HU on expression of mitochondrial morphology and mitochondrial-protein degradation-related genes. Total RNA was prepared from muscle tissues and relative gene expression was determined by real-time PCR. The transcript levels were compared to control mice. The data are means ± SEM ($n = 6$). Statistically significant differences compared to control: $**P < 0.01$ and $***P < 0.001$

Fig. 7 Effects of HU on mRNA expression levels of mitochondrial antioxidant enzyme. Total RNA was prepared from muscle tissues and relative gene expression was determined by real-time PCR. The transcript levels were compared to control mice. The data are means ± SEM ($n = 6$)

mitochondrial fragmentation induced by HU may be caused by down-regulation of mitofusin 2 irrespective of the expression level of fission 1. However, there is direct evidence that over-expression of fission 1 induces mitochondrial fragmentation of myofibers [46]. This study therefore cannot rule out the possibility that fission 1 may contribute to fragmentation of SS mitochondria during HU. In addition, another mitochondria fission-related gene, dynamin 1-like, may play a role in mitochondrial fragmentation during HU.

Unexpectedly, we observed up-regulation of PGC-1α after HU. This finding is inconsistent with that previously reported by Mazzatti et al. [47] who showed decreased expression of PGC-1α after 24 h of HU. This seemingly contradictory finding implies that the response of PGC-1α may differ in the cases of acute and subacute HU. We attribute this discrepancy to the time course of alterations in electromyographic (EMG) activity during HU. The
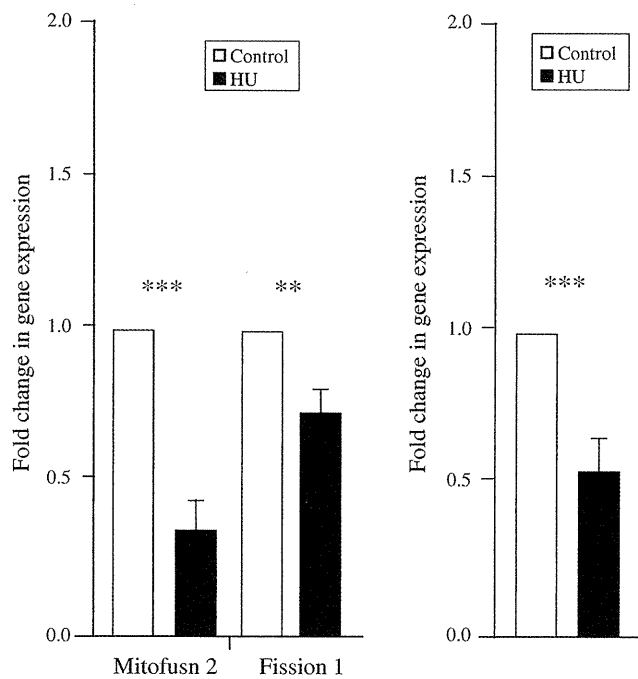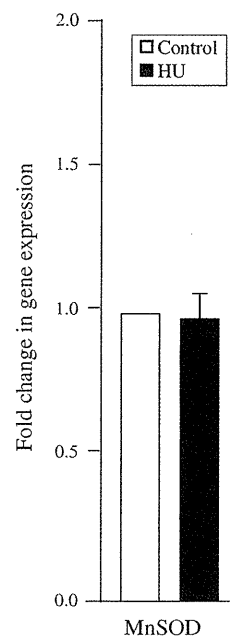
EMG activity of lateral gastrocnemius decreases by half immediately after HU, stays lower than a control levels for 4–5 days, and subsequently tends to recover by 7 days [48], suggesting that recovery of EMG activity may contribute to augmentation of PGC-1α expression as observed

in this study. There may be several potential intracellular signaling pathways by which PGC-1α gene expression could be regulated during HU. First, calcium signaling pathway may contribute to PGC-1α gene expression because HU promotes Ca^{2+} accumulation in myofibers [49]. Calcium/calmodulin-dependent protein kinase IV likely induces PGC-1α expression by activating cyclic-AMP-responsive-element-binding protein (CREB), which in turn binds to a conserved CRE in the PGC-1α promoter [50]. This pathway is also driven by calcineurin A through myocyte enhancer factor 2, which is a potent *trans*-activator of PGC-1α transcription in skeletal muscle [50]. Interestingly, expression levels of calcineurin mRNA and protein are elevated with HU [51]. Therefore, increased expression of PGC-1α during HU may be explained, at least in part, by activating calcium signaling. Second, HU leads to release of catecholamines [52] that can activate β-adrenergic receptors in skeletal muscle [53]. Activation of these receptors increases intracellular cAMP levels and potentially could activate CREB function on the PGC-1α promoter in skeletal muscle as it does in liver [54]. However, because levels of catecholamine were peaked at 12 h after HU, it is uncertain whether catecholamine-mediated pathway contributes to increased expression of PGC-1α as observed in this study. Third, PGC-1α is also induced via cGMP-dependent signaling resulting from elevated levels of nitric oxide (NO) [55]. It has recently been reported that NO and AMP-activated protein kinase (AMPK) act synergistically to up-regulate PGC-1α mRNA expression in vitro [56]. However, HU decreases expression levels of neuronal nitric oxide synthase protein and mRNA [57] while it increases AMPK activity [58]. Therefore, it remains uncertain as to whether the synergistic effect of NO and AMPK on PGC-1α expression during HU. It is very likely that other signaling cascades also may contribute to PGC-1α expression during HU. Further study would be needed to elucidate the possible mechanisms controlling PGC-1α expression during HU.

It is generally assumed that during HU, expression of genes involved in lipid metabolism is decreased, whereas expression of genes involved in glycolytic enzymes and glycogen synthesis is increased. This hypothesis suggests that switching between lipid usage and carbohydrate usage occurs to meet the metabolic demands of the myofibers during HU. In contrast to PGC-1β and PRC, which were down-regulated by HU, PGC-1α was up-regulated concomitant with decreased expression of its DNA binding transcription factors, PPARα and ERRα, which potently induce fatty-acid oxidation genes, MCAD and carnitine palmitoyltransferase I [59, 60]. Our findings may indicate that PGC-1α does not function harmoniously as a coactivator owing to down-regulation of PPARα and ERRα, leading to reduced expression of fatty-acid metabolism-related genes. This hypothesis may be supported by our results (Fig. 7) and previous articles reports that hindlimb suspension down-regulates gene expression of proteins involved in fatty-acid oxidation [34, 61]. Furthermore, we observed that HU decreased the activity of 3-HAD involved in the β-oxidation of fatty acids. Indeed, Grichko et al. [62] reported that fatty-acid oxidation by isolated mitochondria after 2 weeks of hindlimb suspension is on a declining trend although the difference failed to attain statistical significance. Because our result and previous study [42] show that HU decreases the absolute volumes of mitochondria, we suppose that it may also reduce fatty-acid oxidation of myofibers.

It is well established that TFAM plays a key role in mammalian mtDNA transcription/replication [16], whereas mtSSB contributes to its replication, repair, and recombination [63]. There was no alteration in expression of NRF-1, which is activated by PGC-1α and ERRα but expression of its downstream target gene, TFAM was down-regulated after HU. This down-regulation could contribute to mitochondrial dysfunction by reducing template availability for transcription and translation of key mitochondrial proteins. We observed up-regulation of mtSSB concomitant with moderately increased expression of NRF-2, which is shown to potently activate human mtSSB gene expression [64]. It was shown that mtDNA may accumulate more oxidative DNA damage relative to nuclear DNA [65]. mtSSB up-regulation may therefore be a compensatory response to oxidative stress-induced mtDNA damage during HU.

Lon protease level in skeletal muscle decreases with oxidative stress [66]. Because HU increases oxidative stress [67, 68], our finding may be explained by the oxidative stress induced by HU. This study is, to the best of our knowledge, the first to deal with the potential regulation of Lon protease after HU. It is also possible that down-regulation of Lon protease may be responsible for the accumulation of oxidatively damaged proteins within mitochondria, resulting in impairment of mitochondrial function. For example, aconitase, Kreb's cycle enzyme, is one of many mitochondrial matrix proteins that are preferentially degraded by Lon protease after oxidative modification [69]. In addition to the role of protein degradation, Lon protease can also act as a chaperone independently of its proteolytic activity [19], participate in the regulation of mitochondrial gene expression and genome integrity [70, 71], and regulate apoptotic cell death [19], suggesting that Lon protease may play some role in mitochondrial adaptations to HU. Accordingly, further studies are required to elucidate the role of Lon protease in mitochondrial adaptations to HU.

Besides being the primary site of fuel metabolism and ATP production, mitochondria are also a primary source of ROS. Mitochondria also signal, via ROS and Ca^{2+}, and are

critical regulators of cell death pathways [1]. We measured the expression of MnSOD, a primary mitochondrial antioxidant enzyme involved in quenching ROS concentrations. We hypothesized that if mitochondria of HU mice had a greater antioxidant enzyme activity, this could serve to offset elevated ROS production and reduce ROS-induced damage within mitochondria. However, we found no difference in the expression of MnSOD. This observation is in agreement with previous study reported by Andrianjafiniony et al. [72], who found no change in MnSOD activity after 14 days of HU. This does not preclude the possibility that other antioxidant enzymes may be expressed during HU. Indeed, the activities of copper–zinc superoxide dismutase and catalase are increased in hindlimb-unloaded rat [72]. The lack of adaptation of MnSOD activity to increased oxidative stress by HU suggest that a balance between respiration and ROS generation in mitochondria may be lost, leading to mitochondria-mediated apoptosis. Apoptosis can be evoked by ROS-induced mitochondrial release of the proapoptotic proteins. IMF mitochondria release a great amount of cytochrome c and apoptosis-inducing factor in response to oxidative stress compared with SS mitochondria [73], suggesting that not all mitochondria within a myofiber behave similarly. Given that IMF mitochondria were slowly decreased than SS mitochondria during HU, IMF mitochondria may play a major role in initiating apoptosis.

In conclusion, HU distorts gene expression concerning mitochondrial biogenesis, mitochondrial morphogenesis, and mitochondrial-protein degradation, resulting in changes in the abundance, morphology, and functional properties of mitochondria. Unexpectedly, PGC-1α expression is up-regulated after HU. It is unlikely that the augmentation would contribute to mitochondrial biogenesis, because several genes controlled by PGC-1α are down-regulated, suggesting that coordinated expression of PGC-1 family coactivators and DNA binding transcription factors is required for maintaining mitochondrial biogenesis in skeletal muscle. Furthermore, down-regulation of mitochondrial morphology-related genes associated with HU may be also involved in alterations in intracellular mitochondrial distribution. Our findings provide insight into the mitochondrial adaptation in skeletal muscle to HU. Interestingly, Romanello et al. [46] suggest that mitochondrial remodeling contributes to muscle atrophy. Mitochondrial adaptations may therefore have to be considered as an important event when interpreting the results of HU experiments.

References

1. Hock MB, Kralli A (2009) Transcriptional control of mitochondrial biogenesis and function. Annu Rev Physiol 71:177–203
2. Hood DA (2001) Invited review: contractile activity-induced mitochondrial biogenesis in skeletal muscle. J Appl Physiol 90:1137–1157
3. Booth FW (1982) Effect of limb immobilization on skeletal muscle. J Appl Physiol 52:1113–1118
4. Thomason DB, Booth FW (1990) Atrophy of the soleus muscle by hindlimb unweighting. J Appl Physiol 68:1–12
5. Wicks KL, Hood DA (1991) Mitochondrial adaptations in denervated muscle: relationship to muscle performance. Am J Physiol 260:C841–C850
6. Morey-Holton ER, Globus RK (2002) Hindlimb unloading rodent model: technical aspects. J Appl Physiol 92:1367–1377
7. Talmadge RJ (2000) Myosin heavy chain isoform expression following reduced neuromuscular activity: potential regulatory mechanisms. Muscle Nerve 23:661–679
8. Riley DA, Slocum GR, Bain JL, Sedlak FR, Sowa TE, Mellender JW (1990) Rat hindlimb unloading: soleus histochemistry, ultrastructure, and electromyography. J Appl Physiol 69:58–66
9. Yajid F, Mercier JG, Mercier BM, Dubouchaud H, Préfaut C (1998) Effects of 4 wk of hindlimb suspension on skeletal muscle mitochondrial respiration in rats. J Appl Physiol 84:479–485
10. Desplanches D, Mayet MH, Sempore B, Flandrois R (1987) Structural and functional responses to prolonged hindlimb suspension in rat muscle. J Appl Physiol 63:558–563
11. Roy RR, Bello MA, Bouissou P, Edgerton VR (1987) Size and metabolic properties of fibers in rat fast-twitch muscles after hindlimb suspension. J Appl Physiol 62:2348–2357
12. Fell RD, Steffen JM, Musacchia XJ (1985) Effect of hypokinesia-hypodynamia on rat muscle oxidative capacity and glucose uptake. Am J Physiol 249:R308–R312
13. Flynn DE, Max SR (1985) Effects of suspension hypokinesia/hypodynamia on rat skeletal muscle. Aviat Space Environ Med 56:1065–1069
14. Simard C, Lacaille M, Vallières J (1985) Enzymatic adaptations to suspension hypokinesia in skeletal muscle of young and old rats. Mech Ageing Dev 33:1–9
15. Ryan MT, Hoogenraad NJ (2007) Mitochondrial-nuclear communications. Annu Rev Biochem 76:701–722
16. Scarpulla RC (2008) Transcriptional paradigms in mammalian mitochondrial biogenesis and function. Physiol Rev 88:611–638
17. Chen H, Chan DC (2005) Emerging functions of mammalian mitochondrial fusion and fission. Hum Mol Genet 14:R283–R289
18. Ventura-Clapier R, Garnier A, Veksler V (2008) Transcriptional control of mitochondrial biogenesis: the central role of PGC-1alpha. Cardiovasc Res 79:208–217
19. Bota DA, Ngo JK, Davies KJ (2005) Downregulation of the human Lon protease impairs mitochondrial structure and function and causes cell death. Free Radic Biol Med 38:665–677
20. Krieger DA, Tate CA, McMillin-Wood J, Booth FW (1980) Populations of rat skeletal muscle mitochondria after exercise and immobilization. J Appl Physiol 48:23–28
21. Moley-Holtone E, Wronski TJ (1981) Animal models for stimulating weightlessness. Physiologist 24:S45–S48
22. McCarthy JJ, Fox AM, Tsika GL, Gao L, Tsika RW (1997) beta-MHC transgene expression in suspended and mechanically

overloaded/suspended soleus muscle of transgenic mice. Am J Physiol 272:R1552–R1561

23. Srere PA (1969) Citrate synthase. Methods Enzymol 13:3–5

24. Bass A, Brdiczka D, Eyer P, Hofer S, Pette D (1969) Metabolic differentiation of distinct muscle types at the level of enzymatic organization. Eur J Biochem 10:198–206

25. Nachlas MM, Tsou KC, DeSousa E, Cheng CS, Seligman AM (1957) Cytochemical demonstration of succinic dehydrogenase by the use of the new p-nitrophenyl substituted ditetrazole. J Histochem Cytochem 5:420–436

26. van den Bosch BJ, van den Burg CM, Schoonderwoerd K, Lindsey PJ, Scholte HR, de Coo RF, van Rooij E, Rockman HA, Doevendans PA, Smeets HJ (2005) Regional absence of mitochondria causing energy depletion in the myocardium of muscle LIM protein knockout mice. Cardiovasc Res 65:411–418

27. Fischer M, You M, Matsumoto M, Crabb DW (2003) Peroxisome proliferator-activated receptor alpha (PPARalpha) agonist treatment reverses PPARalpha dysfunction and abnormalities in hepatic lipid metabolism in ethanol-fed mice. J Biol Chem 278: 27997–28004

28. Wiwi CA, Gupte M, Waxman DJ (2004) Sexually dimorphic P450 gene expression in liver-specific hepatocyte nuclear factor 4alpha-deficient mice. Mol Endocrinol 18:1975–1987

29. Kraft CS, LeMoine CM, Lyons CN, Michaud D, Mueller CR, Moyes CD (2006) Control of mitochondrial biogenesis during myogenesis. Am J Physiol 290:C1119–C1127

30. Masuyama M, Iida R, Takatsuka H, Yasuda T, Matsuki T (2005) Quantitative change in mitochondrial DNA content in various mouse tissues during aging. Biochim Biophys Acta 1723:302–308

31. Suliman HB, Carraway MS, Welty-Wolf KE, Whorton AR, Piantadosi CA (2003) Lipopolysaccharide stimulates mitochondrial biogenesis via activation of nuclear respiratory factor-1. J Biol Chem 278:41510–41518

32. Schreiber SN, Knutti D, Brogli K, Uhlmann T, Kralli A (2003) The transcriptional coactivator PGC-1 regulates the expression and activity of the orphan nuclear receptor estrogen-related receptor alpha (ERRalpha). J Biol Chem 278:9013–9018

33. Guo Z, Boekhoudt GH, Boss JM (2003) Role of the intronic enhancer in tumor necrosis factor-mediated induction of manganous superoxide dismutase. J Biol Chem 278:23570–23578

34. Stein T, Schluter M, Galante A, Soteropoulos P, Tolias P, Grindeland R, Moran M, Wang T, Polansky M, Wade C (2002) Energy metabolism pathways in rat muscle under conditions of simulated microgravity. J Nutr Biochem 13:471–478

35. Lawler JM, Song W, Demaree SR (2003) Hindlimb unloading increases oxidative stress and disrupts antioxidant capacity in skeletal muscle. Free Radic Biol Med 35:9–16

36. Carlson CJ, Booth FW, Gordon SE (1999) Skeletal muscle myostatin mRNA expression is fiber-type specific and increases during hindlimb unloading. Am J Physiol 277:R601–R606

37. Stelzer JE, Widrick JJ (2003) Effect of hindlimb suspension on the functional properties of slow and fast soleus fibers from three strains of mice. J Appl Physiol 95:2425–2433

38. Stevenson EJ, Giresi PG, Koncarevic A, Kandarian SC (2003) Global analysis of gene expression patterns during disuse atrophy in rat skeletal muscle. J Physiol 551:33–48

39. Bodine SC, Latres E, Baumhueter S, Lai VK, Nunez L, Clarke BA, Poueymirou WT, Panaro FJ, Na E, Dharmarajan K, Pan ZQ, Valenzuela DM, DeChiara TM, Stitt TN, Yancopoulos GD, Glass DJ (2001) Identification of ubiquitin ligases required for skeletal muscle atrophy. Science 294:1704–1708

40. Gomes MD, Lecker SH, Jagoe RT, Navon A, Goldberg AL (2001) Atrogin-1, a muscle-specific F-box protein highly expressed during muscle atrophy. Proc Natl Acad Sci 98:14440–14445

41. Hoppeler H (1986) Exercise-induced ultrastructural changes in skeletal muscle. Int J Sports Med 7:187–204

42. Desplanches D, Kayar SR, Sempore B, Flandrois R, Hoppeler H (1990) Rat soleus muscle ultrastructure after hindlimb suspension. J Appl Physiol 69:504–508

43. Nikawa T, Ishidoh K, Hirasaka K, Ishihara I, Ikemoto M, Kano M, Kominami E, Nonaka I, Ogawa T, Adams GR, Baldwin KM, Yasui N, Kishi K, Takeda S (2004) Skeletal muscle gene expression in space-flown rats. FASEB J 18:522–524

44. Liesa M, Borda-d'Agua B, Medina-Gómez G, Lelliott CJ, Paz JC, Rojo M, Palacín M, Vidal-Puig A, Zorzano A (2008) Mitochondrial fusion is increased by the nuclear coactivator PGC-1beta. PLoS ONE 3:e3613

45. Pich S, Bach D, Briones P, Liesa M, Camps M, Testar X, Palacín M, Zorzano A (2005) The Charcot-Marie-Tooth type 2A gene product, Mfn2, up-regulates fuel oxidation through expression of OXPHOS system. Hum Mol Genet 14:1405–1415

46. Romanello V, Guadagnin E, Gomes L, Roder I, Sandri C, Petersen Y, Milan G, Masiero E, Del Piccolo P, Foretz M, Scorrano L, Rudolf R, Sandri M (2010) Mitochondrial fission and remodelling contributes to muscle atrophy. EMBO J 29:1774–1785

47. Mazzatti DJ, Smith MA, Oita RC, Lim FL, White AJ, Reid MB (2008) Muscle unloading-induced metabolic remodeling is associated with acute alterations in PPARdelta and UCP-3 expression. Physiol Genomics 34:149–161

48. Alford EK, Roy RR, Hodgson JA, Edgerton VR (1987) Electromyography of rat soleus, medial gastrocnemius, and tibialis anterior during hind limb suspension. Exp Neurol 96:635–649

49. Ingalls CP, Warren GL, Armstrong RB (1999) Intracellular Ca2+ transients in mouse soleus muscle after hindlimb unloading and reloading. J Appl Physiol 87:386–390

50. Handschin C, Rhee J, Lin J, Tarr PT, Spiegelman BM (2003) An autoregulatory loop controls peroxisome proliferator-activated receptor gamma coactivator 1alpha expression in muscle. Proc Natl Acad Sci 100:7111–7116

51. Dupont-Versteegden EE, Knox M, Gurley CM, Houlé JD, Peterson CA (2002) Maintenance of muscle mass is not dependent on the calcineurin-NFAT pathway. Am J Physiol 282:C1387–C1395

52. Aviles H, Belay T, Vance M, Sonnenfeld G (2005) Effects of space flight conditions on the function of the immune system and catecholamine production simulated in a rodent model of hindlimb unloading. Neuroimmunomodulation 12:173–181

53. Sakamoto K, Goodyear LJ (2002) Invited review: intracellular signaling in contracting skeletal muscle. J Appl Physiol 93: 369–383

54. Herzig S, Long F, Jhala US, Hedrick S, Quinn R, Bauer A, Rudolph D, Schutz G, Yoon C, Puigserver P, Spiegelman B, Montminy M (2001) CREB regulates hepatic gluconeogenesis through the coactivator PGC-1. Nature 413:179–183

55. Nisoli E, Clementi E, Paolucci C, Cozzi V, Tonello C, Sciorati C, Bracale R, Valerio A, Francolini M, Moncada S, Carruba MO (2003) Mitochondrial biogenesis in mammals: the role of endogenous nitric oxide. Science 299:896–899

56. Lira VA, Brown DL, Lira AK, Kavazis AN, Soltow QA, Zeanah EH, Criswell DS (2010) Nitric oxide and AMPK cooperatively regulate PGC-1 in skeletal muscle cells. J Physiol 588: 3551–3566

57. Tidball JG, Lavergne E, Lau KS, Spencer MJ, Stull JT, Wehling M (1998) Mechanical loading regulates NOS expression and activity in developing and adult skeletal muscle. Am J Physiol 275:C260–C266

58. Hilder TL, Baer LA, Fuller PM, Fuller CA, Grindeland RE, Wade CE, Graves LM (2005) Insulin-independent pathways mediating glucose uptake in hindlimb-suspended skeletal muscle. J Appl Physiol 99:2181–2188

59. Sladek R, Bader JA, Giguère V (1997) The orphan nuclear receptor estrogen-related receptor alpha is a transcriptional

regulator of the human medium-chain acyl coenzyme A dehydrogenase gene. Mol Cell Biol 17:5400–5409

60. Vega RB, Huss JM, Kelly DP (2000) The coactivator PGC-1 cooperates with peroxisome proliferator-activated receptor alpha in transcriptional control of nuclear genes encoding mitochondrial fatty acid oxidation enzymes. Mol Cell Biol 20:1868–1876

61. Wittwer M, Fluck M, Hoppeler H, Muller S, Desplanches D, Billeter R (2002) Prolonged unloading of rat soleus muscle causes distinct adaptations of the gene profile. FASEB J 6: 884–886

62. Grichko VP, Heywood-Cooksey A, Kidd KR, Fitts RH (2000) Substrate profile in rat soleus muscle fibers after hindlimb unloading and fatigue. J Appl Physiol 88:473–478

63. Tomáska L, Nosek J, Kucejová B (2001) Mitochondrial single-stranded DNA-binding proteins: in search for new functions. Biol Chem 382:179–186

64. Bruni F, Polosa PL, Gadaleta MN, Cantatore P, Roberti M (2010) Nuclear respiratory factor 2 induces the expression of many but not all human proteins acting in mitochondrial DNA transcription and replication. J Biol Chem 285:3939–3948

65. Yakes FM, Van Houten B (1997) Mitochondrial DNA damage is more extensive and persists longer than nuclear DNA damage in human cells following oxidative stress. Proc Natl Acad Sci 94:514–519

66. Bota DA, Van Remmen H, Davies KJ (2002) Modulation of Lon protease activity and aconitase turnover during aging and oxidative stress. FEBS Lett 532:103–106

67. Siu PM, Pistilli EE, Alway SE (2008) Age-dependent increase in oxidative stress in gastrocnemius muscle with unloading. J Appl Physiol 105:1695–1705

68. Servais S, Letexier D, Favier R, Duchamp C, Desplanches D (2007) Prevention of unloading-induced atrophy by vitamin E supplementation: links between oxidative stress and soleus muscle proteolysis? Free Radic Biol Med 42:627–635

69. Bota DA, Davies KJ (2002) Lon protease preferentially degrades oxidized mitochondrial aconitase by an ATP-stimulated mechanism. Nat Cell Biol 4:674–680

70. Fu GK, Markovitz DM (1998) The human LON protease binds to mitochondrial promoters in a single-stranded, site-specific, strand-specific manner. Biochemistry 37:1905–1909

71. Langer T, Neupert W (1996) Regulated protein degradation in mitochondria. Experientia 52:1069–1076

72. Andrianjafiniony T, Dupré-Aucouturier S, Letexier D, Couchoux H, Desplanches D (2010) Oxidative stress, apoptosis, and proteolysis in skeletal muscle repair after unloading. Am J Physiol 299:C307–C315

73. Adhihetty PJ, Ljubicic V, Menzies KJ, Hood DA (2005) Differential susceptibility of subsarcolemmal and intermyofibrillar mitochondria to apoptotic stimuli. Am J Physiol 289:C994–C1001

available at www.sciencedirect.com

ScienceDirect

www.elsevier.com/locate/yexcr

Experimental
CELL RESEARCH

ELSEVIER
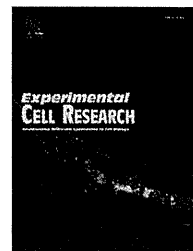
Research Article

IGF-I and vitamin C promote myogenic differentiation of mouse and human skeletal muscle cells at low temperatures

Ai Shima[a], Jennifer Pham[b], Erica Blanco[c], Elisabeth R. Barton[c],
H. Lee Sweeney[b], Ryoichi Matsuda[a],*

[a]Department of Life Sciences, Graduate School of Arts and Sciences, The University of Tokyo, 309A Building 15, 3-8-1 Komaba, Meguro-ku, Tokyo 153-8902, Japan
[b]Department of Physiology, University of Pennsylvania School of Medicine, B701 Richards Building, 3700 Hamilton Walk, Philadelphia, PA 19104, USA
[c]Department of Anatomy and Cell Biology, University of Pennsylvania School of Dental Medicine, 441 Levy Building, 240 S. 40th Street, Philadelphia, PA 19104, USA

ARTICLE INFORMATION

ABSTRACT

In a previous study investigating the effects of low temperature on skeletal muscle differentiation, we demonstrated that C2C12 mouse myoblasts cultured at 30 °C do not express myogenin, a myogenic regulatory factor (MRF), or fuse into multinucleated myotubes. At this low temperature, the myoblasts continuously express Id3, a negative regulator of MRFs, and do not upregulate muscle-specific microRNAs. In this study, we examined if insulin-like growth factor-I (IGF-I) and a stable form of vitamin C (L-ascorbic acid phosphate) could alleviate the low temperature-induced inhibition of myogenic differentiation in C2C12 cells. Although the addition of either IGF-I or vitamin C alone could promote myogenin expression in C2C12 cells at 30 °C, elongated multinucleated myotubes were not formed unless both IGF-I and vitamin C were continuously administered. In human skeletal muscle cells, low temperature-induced blockage of myogenic differentiation was also ameliorated by exogenous IGF-I and vitamin C. In addition, we demonstrated that satellite cells of IGF-I overexpressing transgenic mice in single-fiber culture expressed myogenin at a higher level than those of wild-type mice at 30 °C. This study suggests that body temperature plays an important role in myogenic differentiation of endotherms, but the sensitivity to low temperature could be buffered by certain factors in vivo, such as IGF-I and vitamin C.

© 2010 Elsevier Inc. All rights reserved.

Introduction

Endotherms are able to maintain constant core body temperatures (36–39 °C, [1]) regardless of the surrounding environmental temperature. The high and constant body temperature has resulted in a finely tuned metabolism and high muscular power output in comparison with ectotherms [2]. However, human body temperature actually varies considerably from part to part; for

example, it was reported that the temperature of fingertips is 9 °C lower than the core body temperature (37 °C) in human at room temperature (20 °C) [3].

We have previously examined the effects of low temperature on cell differentiation using skeletal muscle cells as they are distributed throughout the entire body and are expected to be more influenced by surrounding temperature than cells of other organs located deeper inside the body. At a temperature of 30 °C, mouse myoblasts could neither express myogenin, a myogenic regulatory factor (MRF), nor fuse into multinucleated myotubes, and were observed to continuously express Id3, an inhibitory transcription factor for MRFs [4]. Although these results indicate that temperature plays an important role in myogenic differentiation, but there is still a question whether the myocytes completely lose the capacity to differentiate at 30 °C or whether they can differentiate even at low temperature if appropriate rescuers are added to the cell culture.

It is well known that insulin-like growth factor-I (IGF-I) plays multiple important roles during myogenesis by stimulating both growth and differentiation [5]. Transgenic mice which over-express IGF-I in skeletal muscles display promoted adult muscle regeneration and hypertrophy via activation of muscle satellite cells [6–8]. Although there are no reports indicating that IGF-I is capable of inducing myogenin expression at low temperature, we prospected that IGF-I was a good candidate for promoting myogenin expression at 30 °C because it accelerates terminal myogenic differentiation by inducing myogenin expression at normal temperature [9,10]. We were additionally interested in examining IGF-II, as it also binds to IGF-I receptors [11] and induces accelerated myogenic differentiation when overexpressed [12].

Another molecule which affects myogenic differentiation is L-ascorbic acid (vitamin C (VC)). VC plays various essential roles *in vivo*, which includes serving as a cofactor for the hydroxylation of proline and lysine during collagen synthesis. Although L-ascorbic acid is unstable and rapidly degraded under the normal culture conditions [13], a phosphate derivative of L-ascorbic acid is considerably stable, with 85% still remaining after a 1-week incubation at 37 °C [14]. L-ascorbic acid phosphate was reported to increase myogenin expression in muscle cells and promote their myogenic differentiation by accelerating collagen synthesis at 37 °C [15,16]. In this study, we therefore used L-ascorbic acid phosphate instead of L-ascorbic acid as a VC source.

Here, we examined if IGFs (IGF-I and IGF-II) and VC could promote myogenic differentiation at lower temperatures than the normal body temperature of endotherms in C2C12 mouse myoblast cell line, satellite cells on mouse myofibers, and human skeletal muscle cells by immunostaining for myogenin and sarcomeric myosin heavy chain (MyHC) and RT-PCR for myogenin, Id3, and muscle-specific microRNAs (miRNAs). All the results suggested that IGF and VC could promote myogenic differentiation at low temperatures.

Materials and methods

Cell culture

The C2C12 cell line (ATCC, Manassas, VA) [17], which is a subclone of the C2 cell line isolated from the thigh muscle of an adult C3H mouse

[18], was cultured in DMEM (high-glucose) (Nacalai Tesque, Kyoto, Japan) containing 20% FBS (SAFC Biosciences, Lenexa, KS), 50 U/ml penicillin and 50 μg/ml streptomycin on plastic dishes (AGC Techno Glass, Chiba, Japan) coated with 1% bovine skin gelatin (Sigma-Aldrich, St. Louis, MO) at 38 °C in 5% CO_2. At a point of near confluence, the medium was replaced with differentiation medium (DM) which consisted of MEM (Invitrogen, Carlsbad, CA) containing 10% horse serum (Invitrogen) and appropriate antibiotics and the cells were then cultured at either 25, 28, 30 or 38 °C. For rescue experiments, 10, 50 or 100 ng/ml IGF-I (R&D Systems, Minneapolis, MN), 100 ng/ml IGF-II (R&D Systems), or 200 μM L-ascorbic acid phosphate magnesium salt *n*-hydrate (Wako Pure Chemical Industries, Osaka, Japan) was added to DM. The medium was changed every other day.

Conditioned medium (CM) was collected every other day from well differentiated C2C12 cells cultured in DM at 38 °C and passed through 0.22 μm filter to exclude living cells. C2C12 cells were cultured in CM at 30 °C and the medium was changed with fresh CM every other day.

A human skeletal muscle biopsy was obtained under an IRB approved protocol at Children's Hospital of Philadelphia. Explant culture of the biopsy was then performed following the protocol of Decary et al. [19]. Myoblasts obtained from the explant cultures were used to produce immortalized clonal lines, following the procedures of Zhu et al. [20]. Human skeletal muscle cells were cultured in F-10 (Invitrogen) containing 20% FBS and appropriate antibiotics on plastic dishes coated with collagen I (AGC Techno Glass) at 38 °C. At a point of near confluence, the medium was replaced with the identical DM used in the C2C12 culture and the cells were then cultured at either 30 or 38 °C. Rescue experiments using IGF-I and VC were performed as described above for the C2C12 cells.

Single-fiber culture

Single muscle fibers of MLC/mIgf-1 transgenic (IGF-I Tg) mice (see [8], however, donors were not FBV but C57BL/6 mice) and C57BL/6 wild-type (WT) mice were prepared as described previously [21]. Briefly, the extensor digitorum longus (EDL) muscles were removed from euthanized adult male mice by excising the tendons, and were then treated with 0.1% collagenase type I (Sigma-Aldrich) in DMEM at 37 °C for 2 h. The fibers were cultured in DMEM (high-glucose, GlutaMAX-I+) (Invitrogen) containing 20% FBS (Thermo Fisher Scientific, Waltham, MA) and appropriate antibiotics at 37 °C for 3 days (37 °C culture) or at 37 °C for 1 day and then 30 °C for 3 more days (30 °C culture). Animal experimentation was carried out according to the guidelines of the Institutional Animal Care and Use Committee of the University of Pennsylvania.

Immunofluorescence

Immunofluorescence was performed as described previously [4]. Briefly, cells or mouse muscle fibers were fixed with 10% formalin in PBS and treated with 100% methanol. The samples were then incubated with primary antibodies (mouse anti-myogenin, F5D (1:1, Developmental Studies Hybridoma Bank, Iowa City, IA), mouse anti-sarcomeric myosin heavy chain, MF20 (1:2, Developmental Studies Hybridoma Bank) and rabbit anti-MyoD (1:50, Santa Cruz Biotechnology, Santa Cruz, CA)) for 1 h, followed by Alexa Fluor dye-conjugated secondary antibodies (1:400,

Invitrogen) for 1 h. Cell nuclei were stained with either Hoechst 33258 (Sigma-Aldrich) or DAPI (Vector Laboratories, Burlingame, CA).

mRNA isolation and RT-PCR

Total RNA was isolated from C2C12 cells 4 days after the induction of differentiation using RNAZol B reagent (Tel-Test, Friendswood, TX) in accordance with the manufacturer's protocol. Reverse transcription of the isolated mRNA and amplification of cDNA were performed with 100 ng RNA using the SuperScript III One-Step RT-PCR System with Platinum *Taq* DNA Polymerase (Invitrogen). The PCR conditions were 94 °C for 15 s, 60 °C for 30 s, and 55 °C for 45 s for 23 cycles. The sequences of the primers for myogenin, Id3 and β-actin were as follows: myogenin 5'-GAG CTG TAT GAG ACA TCC CC-3' and 5'-GTA AGG GAG TGC AGA TTG TG-3' [22]; Id3 5'-ACT CAG CTT AGC CAG GTG GA-3' and 5'-CAT TCT CGG AAA AGC CAG TC-3'; β-actin 5'-TGG AAT CCT GTG GCA TCC ATG AAA C-3' and 5'-TAA AAC GCA GCT CAG TAA CAG TCC G-3' [23]. The PCR products were resolved by electrophoresis on 2% agarose gels and stained with 1 μM SYTO60 Red Fluorescent Nucleic Acid Stain (Invitrogen) for 20 min. Band intensity was measured using the Odyssey Infrared Imaging System (LI-COR Biosciences, Lincoln, NE). The individual band intensity of myogenin and Id3 was standardized to that of β-actin in the same culture condition.

MiRNA isolation and RT-PCR

Small RNAs were isolated from C2C12 cells 4 days after the induction of differentiation using a *mir*Vana miRNA Isolation Kit (Ambion, Austin, TX, USA) in accordance with the manufacturer's protocol. Reverse transcription of the isolated small RNAs and amplification of cDNA were performed with 10 ng RNA using a *mir*Vana qRT-PCR miRNA Detection Kit (Ambion) and *mir*Vana qRT-PCR Primer Sets (Ambion). The primers for microRNA (miR)-1, miR-133a, miR-181a, miR-206 and 5S rRNA were hsa-miR-1, hsa-miR-133a, hsa-miR-181a, hsa-miR-206 and 5S, respectively. The PCR conditions were 95 °C for 15 s and 60 °C for 30 s for 20 cycles. The PCR products were resolved by electrophoresis on 3.5% agarose gels and stained with 1 μM SYTO60 dye for 20 min. Band intensity was measured using the Odyssey Infrared Imaging System. The individual band intensity of each miRNAs was standardized to that of 5S rRNA in the same culture condition.

Statistical analysis

The cell nuclei expressing myogenin in the C2C12 and human skeletal muscle cells were counted in 3 or 4 different fields for each sample (totaling over 600 nuclei) and the percentages of myogenin-positive nuclei out of the total nuclei were calculated. The cell nuclei in MyHC-positive C2C12 cells were counted in more than 3 different fields for each sample (totaling over 400 nuclei) and the percentages to the total nuclei were calculated. For the single-fiber culture analysis, the ratios of myogenin-positive nuclei to MyoD-positive nuclei per myofiber were calculated. The number of analyzed myofibers was as follows: in the 37 °C culture, IGF-I Tg: $n = 52$, WT: $n = 34$ (day 2), IGF-I Tg: $n = 46$, WT: $n = 37$ (day 3); in the 30 °C culture, IGF-I Tg: $n = 61$, WT: $n = 37$ (day 3), IGF-I Tg: $n = 45$, WT: $n = 29$ (day 4). The percentages or ratios are presented as the mean ± SEM. The Student's *t*-test was used to analyze statistical significance.

Results

IGF-I and VC promote myogenin expression and myotube formation of C2C12 cells at 30 °C

At 38 °C, which is close to the normal body temperature of a mouse, C2C12 mouse myoblast cells undergo terminal differentiation immediately after being switched to DM and fuse into multinucleated myotubes. At 30 °C, however, myoblast cells express MyoD, but not myogenin, and do not form myotubes [4]. To elucidate that the lack of differentiation at low temperature was only due to temporary blocking and not a complete loss of the capacity to differentiate, we searched for factors that could promote myotube formation at 30 °C.

C2C12 cells in DM containing either IGF-I or L-ascorbic acid phosphate, a stable form of VC, expressed myogenin 4 days after the induction of differentiation (day 4) (Fig. 1A) and fused into myotubes by day 6 at 30 °C (Fig. 1B). Although the treatment with 100 ng/ml IGF-I or 200 μM VC promoted myogenin expression independently, the effect was synergetically enhanced when they were added in combination. Cells cultured in DM containing both IGF-I and VC formed multinucleated myotubes expressing MyHC, while only mononucleated myocytes or thinner myotubes were observed in DM containing IGF-I or VC alone (Fig. 1B). The percentage of nuclei in the MyHC-positive cells to the total nuclei was also significantly higher in the culture containing both IGF-I and VC than that in the culture containing either IGF-I or VC alone (Fig. 1C). IGF-I promoted myogenin expression in a dose-dependent manner, when the VC concentration was fixed at 200 μM (Fig. 1D). To examine whether the continuous addition of IGF-I was required to promote myogenic differentiation at 30 °C, the period of IGF-I treatment was changed while 200 μM VC was maintained in the medium throughout the culture. The treatment of 100 ng/ml IGF-I for only 1 or 2 days after the induction of differentiation could not promote the expression of myogenin at 30 °C (Fig. 1E), suggesting that the continuous presence of IGF-I for several days was required.

IGF-II also promotes myogenic differentiation at 30 °C

We also examined whether the addition of IGF-II, a homologue of IGF-I, could promote myogenic differentiation at 30 °C with or without the presence of VC. The percentage of myogenin-expressing nuclei to the total nuclei was higher when both IGF-II and VC were used to treat myoblasts than IGF-II alone (Fig. 2A). However, the percentage of myogenin-positive nuclei (11% ± 1.2 (−VC), 19% ± 3.2 (+VC)) was generally lower than that observed in IGF-I-treated cells (16% ± 0.8 (−VC), 33% ± 1.1 (+VC)) when the IGFs were added at identical concentrations (100 ng/ml). Multinucleated myotubes were formed in DM containing both IGF-II and VC, while thinner myotubes were formed when only IGF-II was added to DM (Fig. 2B and C).

Id3 expression is downregulated by IGF-I and VC

In a previous study [4], we reported that Id3, which acts as a negative regulator of MRFs and is downregulated upon the initiation of differentiation at 38 °C [24], was continuously expressed in myoblasts at 30 °C. Here, we examined whether the
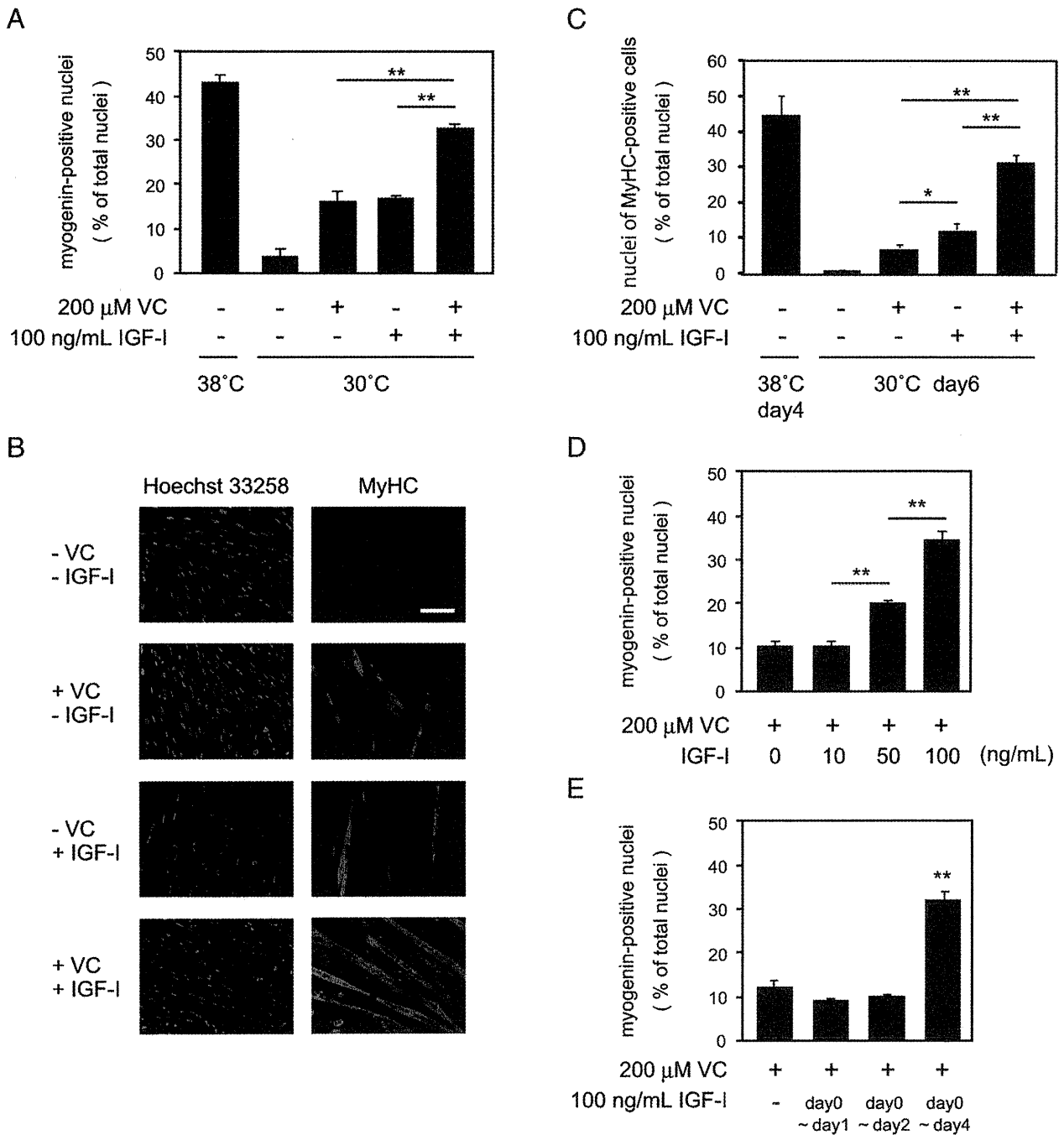
Fig. 1 – Effects of IGF-I and VC on myogenic differentiation of C2C12 cells at 30 °C. A. C2C12 cells were cultured in DM at either 38 or 30 °C and in DM containing 100 ng/ml IGF-I or 200 μM VC at 30 °C for 4 days prior to immunostaining for myogenin. Myogenin expression of the cells cultured in DM with both IGF-I and VC was significantly higher than that of the cells in DM with either IGF-I or VC alone. The percentages of myogenin-positive nuclei to the total nuclei are presented as the mean ± SEM. $**p < 0.01$. B. C2C12 cells were cultured in DM with or without 100 ng/ml IGF-I and 200 μM VC at 30 °C for 6 days prior to immunostaining for MyHC. Cell nuclei were stained with Hoechst 33258. Thick multinucleated myotubes were formed in DM containing both IGF-I and VC, but only mononucleated myocytes or thinner myotubes expressed MyHC in DM with either IGF-I or VC alone. Scale bar: 100 μm. C. The percentages of nuclei in MyHC-positive cells to the total nuclei were determined by the immunostaining of C2C12 cells cultured at 38 °C for 4 days or at 30 °C for 6 days. MyHC expression of the cells cultured in DM with both IGF-I and VC at 30 °C was significantly higher than that of the cells in DM with either IGF-I or VC alone at 30 °C. $**p < 0.01$. $*p < 0.05$. D. C2C12 cells were cultured in DM with 0, 10, 50, 100 ng/ml IGF-I and 200 μM VC at 30 °C for 4 days. IGF-I rescued myogenin expression in a dose-dependent manner. $**p < 0.01$. E. The IGF-I treatment period was changed during the C2C12 culture with 200 μM VC at 30 °C for 4 days; no treatment (-), treatment from day 0 to day 1 (1 day), from day 0 to day 2 (2 days) or from day 0 to day 4 (4 days). The exposure to IGF-I for only 1 or 2 days could not promote myogenin expression. $**p < 0.01$ vs. 3 other conditions.
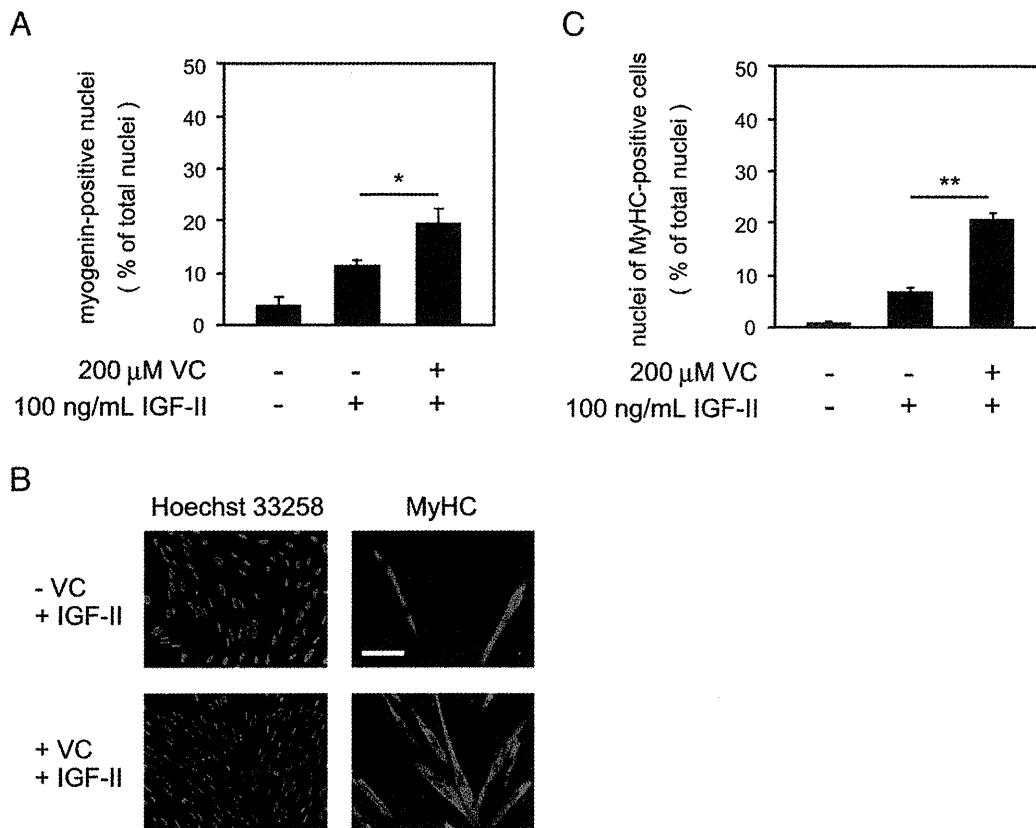
Fig. 2 – Effects of IGF-II and VC on myogenic differentiation of C2C12 cells at 30 °C. A. C2C12 cells were cultured in DM with or without 100 ng/ml IGF-II and 200 μM VC at 30 °C for 4 days and then immunostained for myogenin. Myogenin expression of the cells cultured in DM with both IGF-II and VC was significantly higher than that of the cells cultured in DM with IGF-II alone. The percentages of myogenin-positive nuclei to the total nuclei are presented as the mean ± SEM. $^*p < 0.05$. B. C2C12 cells were cultured in DM with or without 100 ng/ml IGF-II and 200 μM VC at 30 °C for 6 days and then immunostained for MyHC. Cell nuclei were stained with Hoechst 33258. The cells in DM containing both IGF-II and VC formed numerous multinucleated myotubes, but only thin myotubes were observed in DM containing IGF-II alone. Scale bar: 100 μm. C. The percentages of nuclei in MyHC-positive cells to the total nuclei were determined by the immunostaining of C2C12 cells cultured at 30 °C for 6 days. MyHC expression of the cells cultured in DM with both IGF-II and VC was significantly higher than that of the cells in DM with IGF-II alone. $^{**}p < 0.01$.

addition of IGF-I and VC would result in the decreased expression of Id3 at 30 °C. RT-PCR was used to examine the expression profiles of C2C12 cells cultured in either DM without adding IGF-I nor VC (DM(−)) at 38 and 30 °C or DM containing both 100 ng/ml IGF-I and 200 μM VC at 30 °C (Fig. 3).The individual band intensity of myogenin and Id3 was measured and standardized to that of β-actin in the same condition (Table 1). The presence of IGF-I and VC increased myogenin expression and decreased Id3 expression at 30 °C compared with those of the cells cultured in DM(−) (Fig. 3).

Expressions of muscle-specific miRNAs are upregulated by IGF-I and VC

Our previous study examining the temperature-dependent expression of the muscle-specific miRNAs miR-1, -133a, -181a, and -206 revealed that they were upregulated at 38 °C but not at 30 °C [4]. These miRNAs are specifically expressed or highly enriched in skeletal muscles and regulate myogenic differentiation [25]. RT-PCR revealed that the C2C12 cells cultured in DM containing both 100 ng/ml IGF-I and 200 μM VC at 30 °C expressed all of these miRNAs at nearly identical levels as the cells cultured in DM(−) at
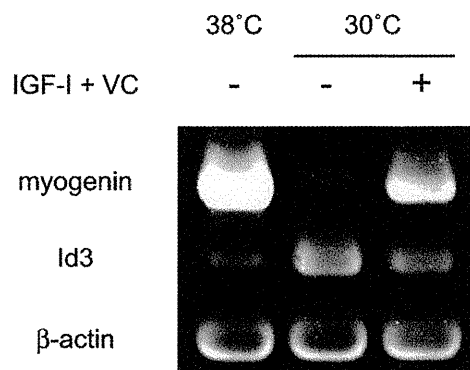

Fig. 3 – RT-PCR of myogenin and Id3 in C2C12 cells. Total RNA was isolated from C2C12 cells cultured in DM at 38 or 30 °C and in DM containing 100 ng/ml IGF-I and 200 μM VC at 30 °C for 4 days. IGF-I and VC increased myogenin expression and decreased Id3 expression at 30 °C compared with cells cultured without IGF-I or VC.

Table 1 – Band intensity of myogenin and Id3.

IGF-I + VC	38 °C	30 °C	
	—	—	+
Myogenin	3.13	0.21	1.43
Id3	0.35	1.00	0.55

Table 2 – Band intensity of microRNAs.

IGF-I + VC	38 °C	30 °C	
	—	—	+
miR-1	0.87	0.17	0.83
miR-133a	1.11	0.21	0.80
miR-181a	0.36	0.16	0.36
miR-206	1.04	0.22	0.92

38 °C (Fig. 4). The muscle-specific miRNAs were barely detectable in the cells cultured in DM(−) at 30 °C, though they expressed the 5S rRNA internal standard at levels similar to the cells cultured at 38 °C (Fig. 4). The individual band intensity of each miRNAs was measured and standardized to that of 5S rRNA in the same condition (Table 2).

IGF-I and VC can promote myogenic differentiation at temperatures lower than 30 °C

As IGF-I and VC were both shown to be able to prevent the low temperature-induced inhibition of myogenic differentiation, the ability of these factors to promote muscle cell differentiation at temperatures lower than 30 °C was examined. C2C12 cells were cultured in DM containing both 100 ng/ml IGF-I and 200 μM VC at either 25 or 28 °C and then immunostained for myogenin and MyHC. At both temperature, IGF-I and VC promoted expression of myogenin and MyHC (Fig. 5A and B), while no myoblasts expressed them when cultured in DM(−). Multinucleated myotubes were formed by day 10 at 28 °C, while only mono- or bi-nucleated myocytes were observed on day 11 at 25 °C (Fig. 5C).
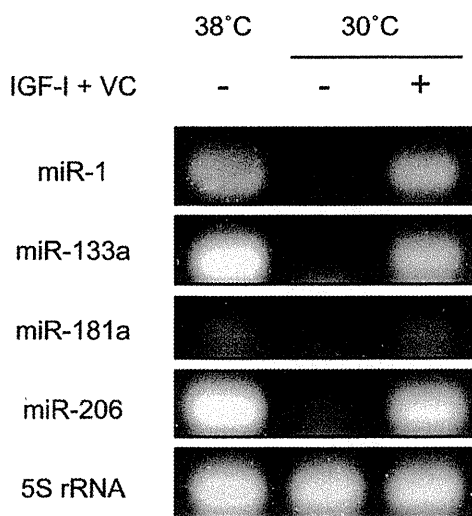

Fig. 4 – RT-PCR of muscle-specific miRNAs in C2C12 cells. Small RNAs were isolated from C2C12 cells cultured in DM at 38 or 30 °C and in DM with 100 ng/ml IGF-I and 200 μM VC at 30 °C for 4 days. RT-PCR for the muscle-specific miRNAs miR-1, -133a, -181a and -206 revealed that the cells cultured in DM with IGF-I and VC at 30 °C expressed all of these miRNAs at nearly identical levels as the cells cultured at 38 °C. The control cells cultured in DM(−) at 30 °C expressed 5S rRNA, the internal standard, but hardly expressed the muscle-specific miRNAs.

Satellite cells of IGF-I overexpressing Tg mice swiftly differentiate at both 37 °C and 30 °C

Satellite cells are myogenic stem cells [26] that are activated by signals released from crushed myofibers [27] to differentiate into myotubes which contribute to muscle regeneration [28]. In a previous study, we demonstrated that activated satellite cells expressed MyoD but not myogenin at 30 °C by day 3 [4]. Here, after the isolation of myofibers from IGF-I Tg mice, which display postnatal increases in muscle mass and strength [8], myogenin expression in the satellite cells was compared with the levels in WT mice without VC in 37 °C and 30 °C cultures. For both experimental conditions, myofibers were cultured at 37 °C for the initial 24 h in order to activate the satellite cells. To evaluate myogenin expression in satellite cells, we calculated the ratio of myogenin-positive nuclei to MyoD-positive nuclei per myofiber. A ratio greater than 1.0 indicated that a majority of satellite cells expressed myogenin, but had already downregulated MyoD expression. In the 37 °C culture, the ratio of myogenin-positive cells in IGF-I Tg mice was higher than that of WT mice on day 2, which suggests that the myogenic differentiation of satellite cells of IGF-I Tg mice was accelerated in comparison with WT mice. However by day 3, the difference in the ratios of myogenin-positive cells between IGF-I Tg mice and WT mice had disappeared (Fig. 6A). In the 30 °C culture, very few satellite cells of both IGF-I Tg and WT mice expressed myogenin on day 3, but on day 4, the ratio of myogenin-positive satellite cells of IGF-I Tg mice was significantly higher level than that of WT mice (Fig. 6B). A number of satellite cells of WT mice, however, expressed myogenin at 30 °C on day 4 (Fig. 6B and C), which was different from the observed expression pattern in C2C12 cells.

Conditioned medium from differentiated C2C12 cells can promote myogenin expression at 30 °C

We hypothesized that the reason why satellite cells of WT mice expressed myogenin at 30 °C without exogenous IGF-I and VC in the single-fiber culture was that some physiological factors which could rescue myogenin expression at 30 °C were brought or secreted into the medium from the myofibers. Therefore, we examined whether or not conditioned medium (CM) from C2C12 cells differentiated at 38 °C could rescue myogenin expression at 30 °C. C2C12 cells cultured in CM for 6 days expressed myogenin at almost the same level of the culture with 100 ng/ml IGF-I and 200 μM VC at 30 °C (Fig. 7A). The myoblasts cultured in CM at 30 °C expressed MyHC, but did not fuse into multinucleated myotubes even when cultured for 10 days, while the cell density gradually decreased (Fig. 7B).
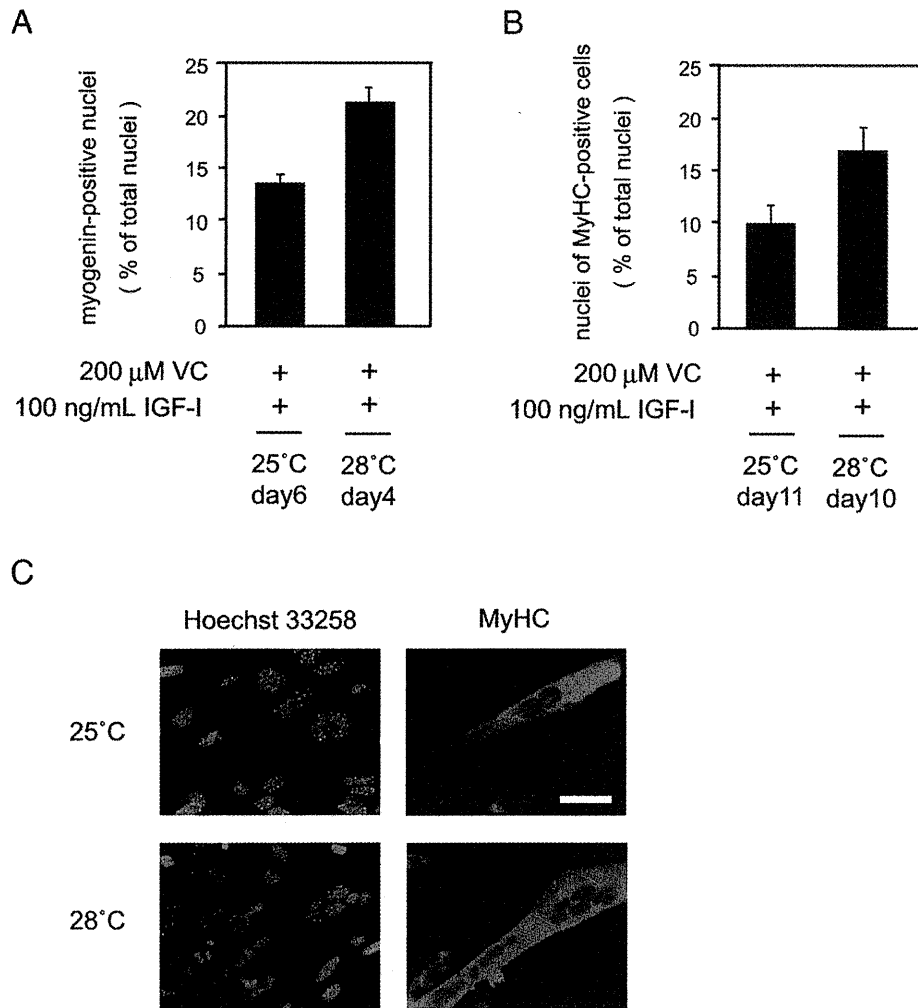
Fig. 5 – Effects of IGF-I and VC on myogenic differentiation of C2C12 cells at 25 and 28 °C. A. C2C12 cells were cultured in DM containing both 100 ng/ml IGF-I and 200 μM VC at 25 °C for 6 days or at 28 °C for 4 days and immunostained for myogenin. The percentages of myogenin-positive nuclei to the total nuclei are presented as the mean ± SEM. B. C2C12 cells were cultured in DM containing both 100 ng/ml IGF-I and 200 μM VC at 25 °C for 11 days or at 28 °C for 10 days and then immunostained for MyHC. The percentages of nuclei in MyHC-positive cells to the total nuclei are presented as the mean ± SEM. C. C2C12 cells were cultured in DM containing both 100 ng/ml IGF-I and 200 μM VC at 25 °C for 11 days or at 28 °C for 10 days and then immunostained for MyHC. Cell nuclei were stained with Hoechst 33258. Although the cells expressed MyHC at both temperatures, multinucleated myotubes were formed only at 28 °C, while mononucleated myocytes or binucleated myotubes were observed at 25 °C. Scale bar: 50 μm.

IGF-I and VC promote myogenic differentiation of human muscle cells at 30 °C

Finally, we examined whether human skeletal muscle cells could also be promoted to differentiate by treatment with IGF-I and VC at 30 °C. Although the percentage of myogenin-positive nuclei of human skeletal muscle cells was generally low (14.1 ± 0.8%) in comparison with C2C12 cells (42.9 ± 1.9%) even at 38 °C, the inhibition of myogenin expression at 30 °C (1.1 ± 0.3%) and the rescue effect with IGF-I and VC (16.2 ± 1.8%) was clearly demonstrated (Fig. 8).

Discussion

Mouse myoblasts do not differentiate into multinucleated myotubes at 30 °C, which is much lower than the core body temperature of most endotherms [4]. In this study, we demon-

strated that at this temperature myoblasts do not completely lose the capacity to differentiate, as the treatment with exogenous IGFs (IGF-I and IGF-II) and VC stimulates myoblasts to proceed toward terminal differentiation. Although the addition of either IGF-I alone or VC alone could promote myogenin expression in C2C12 cells at 30 °C, elongated multinucleated myotubes which had almost the same appearance as the myotubes cultured at 38 °C were not formed unless both 100 ng/ml IGF-I and 200 μM VC were continuously administered over a period of several days. IGF-II, which also binds to IGF-I receptors, showed the same effects on myogenic differentiation at low temperature in the combination with vitamin C. These results show that appropriate chemical factors can overcome the inadequacy of temperature for myogenic differentiation, suggesting that the physical information such as external temperature shares the same downstream signaling pathways with the chemical information such as growth factors.

It is well established that IGF-I promotes both skeletal muscle growth and differentiation [5]. At normal physiological